Hindawi
Journal of Sensors
Volume 2022, Article ID 1855493, 19 pages
https://doi.org/10.1155/2022/1855493

Review Article

NiO-Based Gas Sensors for Ethanol Detection: Recent Progress

Qingting Li,[1] **Wen Zeng**,[1] **and Yanqiong Li**[2]

[1]*College of Materials Science and Engineering, Chongqing University, Chongqing 400030, China*
[2]*School of Electronic Information & Electrical Engineering, Chongqing University of Arts and Sciences, Chongqing 400030, China*

Correspondence should be addressed to Wen Zeng; wenzeng@cqu.edu.cn and Yanqiong Li; 702121437@qq.com

Received 11 June 2022; Revised 26 July 2022; Accepted 28 July 2022; Published 26 August 2022

Academic Editor: Akhilesh Pathak

In this review, we summarized the state-of-the-art progress on the ethanol performance of NiO by means of morphology, doping, loading noble metal particles, and forming heterojunctions. We first introduced the effect of modulating NiO morphology on ethanol performance that has been reported in recent years. The morphology with large specific surface area and high porosity was considered to be the one that can bring high gas response. Then, we discussed the enhanced effect of the doping of metal cations and noble metal particle loading on the ethanol-sensitive properties of NiO. Doping ions increased the ground-state resistance and increased the oxygen defect concentration of NiO. The effects of noble metal particles on the performance of NiO included chemical sensitization and electronic sensitization. Finally, the related contents of NiO forming complexes with metal oxides and bimetallic oxides were discussed. In this section, the specific improvement mechanism was discussed first, and then, the related work of researchers in recent years was summarized. At the same time, we presented a reasonable outlook for NiO-based ethanol sensors, imagining future directions.

1. Introduction

Volatile organic compounds (VOCs) often appear in our lives, such as the smell of gasoline, paint, and nail polish. These VOC gases degrade air quality and even destroy the ozone layer. At the same time, these gases threaten human body [1–3]. For example, ethanol exists in laboratories, medical industries, and industrial production. When exposed to high concentrations of ethanol, humans are prone to adverse symptoms such as skin irritation and headache [4–6]. In order to prevent problems before they occur, it is essential to develop ethanol sensors to monitor ethanol concentration. In addition, ethanol sensors also play an important role in detecting drunk driving [7]. Currently, gas detection technology includes gas chromatography [8], quartz crystal microbalance [9], and TDLAS detection technology [10]. However, real-time monitoring of ethanol is achieved by chemiresistive sensors with the advantages of easy preparation, low cost, and portability [11, 12].

Metal oxide semiconductors (MOS) have special electrical conductivity, good stability, and high gas response [13–15]. ZnO [16–18], SnO_2 [19–21], NiO [22, 23], WO_3 [24–26], In_2O_3 [27–29], etc. are widely used in ethanol gas sensors. For instance, Jiang et al. [16] synthesized an ethanol sensor of mesoporous ZnO nanospheres, which had abundant pore structures and large specific surface area. From the ethanol gas sensing test results, it could be seen that the ZnO sensors achieved a response of 58.4 to 100 ppm ethanol at 250°C. Furthermore, this sensor could detect ppb levels of ethanol, getting a response of 1.17 at 500 ppb ethanol. For the MOS gas sensor, the resistance is used as the measured physical signal to detect the gas. When the MOS is in the air, oxygen molecules adsorb on the surface of the MOS and take electrons out. After the electrons are extracted, the carriers (electrons) of the n-type semiconductor decrease to form an electron depletion layer (EDL), while the carriers (holes) of the p-type semiconductor increase to form a hole accumulation layer (HAL). When the material comes into contact with the reducing ethanol molecules, the electrons captured by oxygen are released back into the sensitive material. The carriers of the n-type semiconductor increase, so the resistance becomes larger; the carriers of the p-type semiconductor decrease, so the resistance becomes smaller [30–32]. In addition to single metal oxides, bimetallic metal oxides have also been used as

gas sensing materials in recent years [33], including $NiCo_2O_4$ [34], $ZnCo_2O_4$ [35], and $LaFeO_3$ [36]. Even though MOS possess the above advantages, high operating temperature and low selectivity are still their bottlenecks as gas sensors [37]. Among them, we often say that there is no selectivity, which means that pure MOS has only a weak gas response to the gas. It is not easy to distinguish it after mixing with other gases. Therefore, if the selectivity is not outstanding, it is considered to be nonselective. Scholars have done a lot of research to overcome these shortcomings, including doping, compounding with other materials, morphology manipulation, and UV activation [38–40]. For example, extensive experiments showed that the loading of Pd particles was important for the H_2 selectivity. Because H_2 adsorbs on Pd to form PdH_x, which not only increased the electrical resistance but also caused the volume expansion of the Pd host. The volume expansion of Pd enabled rapid and highly selective detection of H_2. Polyaniline had high selectivity to NH_3 due to its carbon structure and special protonation/deprotonation process [41, 42]. At the same time, these modification methods can also reduce the temperature of the MOS-based gas sensors, hoping that it can make sensors work at low temperature or even room temperature. For example, ultraviolet light gives the sensor an external energy from the outside, and the energy required for the reaction is not necessarily obtained from the temperature. At the same time, the UV makes the sensitive material generate photogenerated carriers for the gas sensing reaction, which further reduces the temperature and increases the response [43]. The morphology manipulation is often used, such as the hierarchical structures. These hierarchical structures have a large number of pore structures that provide efficient gas diffusion paths, which can enhance gas response and significantly reduce operating temperature [44].

The p-type semiconductor NiO has strong oxidizing properties, excellent catalytic activity, and good electrical conductivity, so it has attracted attention in gas sensors [45, 46]. So far, more than 1,000 reports on NiO materials used in gas sensors have been published, and these reports are mainly concentrated in the past five years. For example, Li et al.'s team [47] fabricated ultrathin $Ni(OH)_2$ nanosheets directly on the substrate without using additional surfactants. The obtained NiO nanosheets had a porous structure, which was favorable for the diffusion of gas molecules. At the same time, the nanosheets provided a large surface area and crystal planes with an affinity for acetone gas. Due to these advantages, the NiO nanosheet sensor had a response value as high as 60% when detecting 100 ppb acetone gas. In addition, the NiO nanosheets exhibited a low LOD of 0.8 ppb for acetone with good stability. However, according to reports, the response of pristine NiO to ethanol was low, so the researchers modified NiO using various methods. These modifications include morphology control, doping, loading of noble metal particles, and formation of composites with n-type semiconductors. According to the survey, there have been many reports on the detection of ethanol by NiO sensors in recent years. However, the rare review on the detection of ethanol by NiO is summarized in the existing reports. Therefore, a review article is needed to systematically introduce the research basis of NiO ethanol sensors, which will help scholars to quickly clarify their ideas and understand the entire research field. In addition, scholars can discover unresolved questions and think about new research directions from this review.

In this review, we will describe the influence of different modification methods on the ethanol sensitivity of NiO and summarize the development level of NiO for ethanol detection in recent years in a tabular form. We first introduced the effect of modified NiO morphology on ethanol performance that has been reported in recent years. The morphology with large specific surface area and high porosity was considered to be the structure that could bring high gas response. Then, we discussed the enhanced effect of the doping of metal cations and noble metal particle loading on the ethanol-sensitive properties of NiO. Doping ions increased the ground-state resistance and the oxygen defect concentration of NiO. The effects of noble metal particles on the performance of NiO included chemical sensitization and electronic sensitization. Finally, the related contents of NiO forming composites with metal oxides and bimetallic oxides were discussed. In this section, the specific improvement mechanism was discussed first, and then, the related work of researchers in recent years was summarized. At the same time, we presented a reasonable outlook for NiO-based ethanol sensors, imagining future directions.

2. Morphology

The gas response goes hand in hand with the specific surface area and porosity of the material [48, 49]. Therefore, researchers' research on topography is based on high specific surface area and porosity. During the study of the morphology, the researchers found that the grain size of the material is an important factor. When the grain size is equal to or less than twice the Debye length ($2\lambda D$), the conductance is highly influenced by each grain. So the gas response is strongly influenced by the grain size. When the grain size is larger than $2\lambda D$, the relationship between the gas response and grain size gradually weakens, and the response becomes independent. But in this case, the conductivity is affected by the Schottky barrier at the grain boundaries [50]. However, compared with studies on grains, recent reports on NiO morphologies have focused on obtaining large specific surface areas and high porosity, such as NiO nanosheets [51–53] and NiO nanoflowers [54–58]. Next, the progress of NiO nanomaterials with different morphologies in ethanol sensing will be introduced.

The 2D structure of nanosheets has remarkably high specific surface area and abundant gas channels, while the spatial confinement endows 2D sensitive materials with unique properties [59–61]. The more target gas molecules attached to the metal oxides surface, the greater the resistance change of the material, that is, the higher the gas response [62]. Besides, the flexibility of 2D metal oxides enables for high compatible integration with flexible substrates, which can be applied in the field of flexible wearable sensors. Therefore, nanosheets with satisfactory sensitive properties are favored by scholars in resistive sensors. Many reports on metal oxide nanosheets have pointed out that fabricating porous surfaces on nanosheets

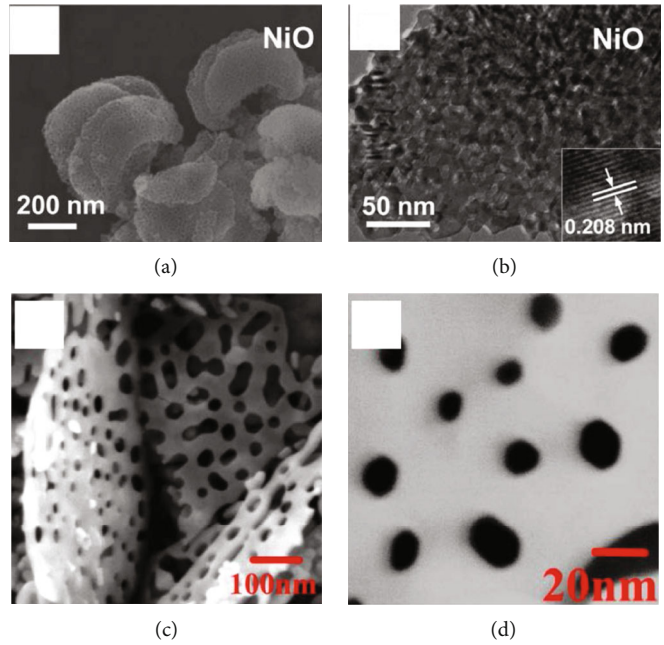

Figure 1: (a) SEM of crescent-shaped NiO nanoplates (reprinted/adapted by [53]). (b) HRTEM of crescent-shaped NiO nanoplates (reprinted/adapted by [53]). (c and d) SEM of NiO lotus root slice (reprinted/adapted by [52]).

could effectively improve their gas sensing properties [63]. Su et al. [53] prepared a new and unique crescent-shaped NiO nanosheet. During the calcination process, the water and gas from the NiO nanosheets were get rid of, resulting in a porous structure (as shown in Figures 1(a) and 1(b)). The steady crescent-shaped structure alleviated the accumulation of nanoparticles, and the mesopores uniformly distributed on the nanosheets improved the gas diffusion channel, making ethanol molecules easier to diffuse into NiO. The gas sensors based on crescent NiO nanosheets could rapidly detect 100 ppm ethanol at 130°C (response time and recovery time was 5 s and 20 s, respectively), with a response as high as 68.1%. At the same time, the LOD showed a low value of 200 ppb by calculation. The authors believed that the excellent ethanol sensitivity gave the credit to its steady porosity structure with tiny particle size and abundant reaction sites. Cao et al. [52] prepared a lotus root-like NiO nanosheet (as shown in Figures 1(c) and 1(d)). The average pore diameter of this lotus root structure was 15-50 nm. The specific surface area of lotus root NiO was 156.485 m^2/g, which was 13 times that of ordinary NiO. Due to this unique morphology, lotus root NiO had a response of 1.51 to 80 ppm ethanol at 300°C.

The hierarchically nanoflowers structured are assembled from nanoneedles and nanosheets. This hierarchical structure is beneficial for gas adsorption and electron transport, which improves the surface reaction efficiency. At the same time, the 3D structure increases the number of its adsorption sites. This novel flower-like structure has been demonstrated to have excellent functions in photoluminescence and photocatalysis [64–66]. Zhang and Zeng [55] investigated the sensitivity of nanoflower gas sensors assembled by nanoneedles and nanosheets to ethanol (Figures 2(a) and 2(b)). Both of them showed excellent gas response to ethanol. Due to the larger specific surface area of nanosheets, which could attract more gas molecules to react, the nanoflower sensors based on nanosheets obtained a larger gas response (the gas response of nanoneedles was 25 and nanosheets was 55). In particular, the authors mentioned that the nanoneedle-based NiO flowers could detect ethanol faster due to the lower potential energy and higher conductivity of the nanoneedles (the response/recovery time of nanoneedles was 1.7/2.2 s and nanosheets was 4.8/7 s). Nanoflowers composed of nanoneedles and nanosheets had their unique advantages, which meant that different morphologies can be synthesized according to specific needs in the future. If the sensor needed a higher response, the nanosheet flower might be a good choice; if the sensor needed to detect the target gas quickly, then the nanoneedle flower was an effective way. In addition to nanoflowers assembled from nanoneedles and nanosheets, Carbone and Tagliatesta [56] reported a granular flower assembled from particles. This granular flower was an aggregate of particles with a diameter of 10 nm (Figure 2(c)), whose surface had a great quantity of electrons that favor surface reactions. At the same time, the sturdy interparticle distance provided a stable surface for gas adsorption. NiO nanoparticles had charge/hole accumulation in short dimensions, which contained more accumulation of defects and traps. Therefore, these several factors led to the excellent ethanol sensing performance. The NiO granular flower sensor had a 35% response to 150 ppm ethanol at 200°C with a response/recovery time of 3/6 s.

It is worth noting that a lot of research have found that the hollow structure will bring a higher specific surface area and more adsorption active sites [67–69]. The interior of the hollow structure can also serve as a microreaction chamber, providing a place for gas molecules to react with sensitive materials, and a short distance for carrier transport. For the hollow structure of NiO, NiO hollow nanofibers [70] and hollow spheres [71–75] have been reported, and they have

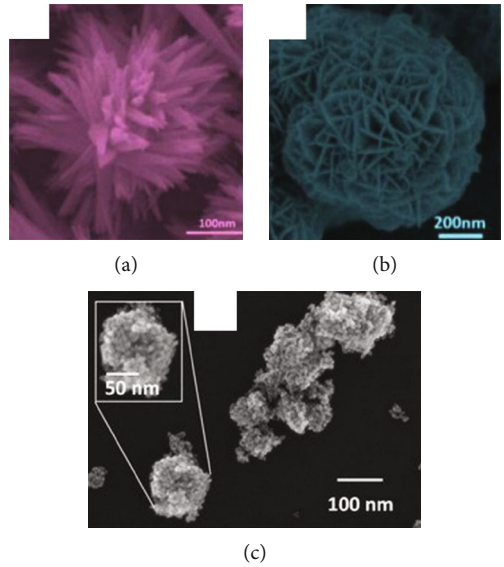

Figure 2: SEM of NiO nanoflower assembled from (a) nanoneedles (reprinted/adapted by [55]), (b) nanosheets (reprinted/adapted by [55]), and (c) nanoparticles [56] (open access).

obtained excellent performance in gas sensing with large specific surface area. In recent years, only NiO hollow spheres have been reported for ethanol gas sensing. Chu et al.'s team [73] used the Kirkendall effect to prepare NiO hollow nanospheres. At 240°C, the NiO hollow sphere-based sensor obtained a response of 3.1 to 800 ppm ethanol. The authors exhibited that the hollow nanostructures had enhanced surface activity, while the hollow shell layer enabled rapid diffusion of ethanol molecules and easy penetration into the interior of sensor. These properties made the hollow structure a new route to realize highly sensitive NiO ethanol sensors.

The exposed surfaces of semiconductor nanomaterials are also of interest to scholars, because different exposed surfaces lead to different surface atomic structures and properties. It has been confirmed by numerous experiments that NiO with exposed {111} facets had excellent sensitive characteristics, which owned to the 3-coordinated unsaturated Ni atoms of the {111} facets. Due to the lack of oxygen and great reducibility, the 3-coordinated Ni atoms can adsorb O_2, bring free electrons, and promote the chemical reaction between oxygen species and ethanol gas [76, 77]. Furthermore, the {111} planes of NiO have a greater number of unsaturated O atoms and a higher surface energy than the usually exposed {220} planes, which is beneficial for sensitive performance [78, 79]. Liu et al. [77] prepared NiO foam structures with exposed {111} and {220} planes, and NiO with exposed {111} planes had fewer surface single-bond H groups and had higher 3-coordinated Ni atomic density. In addition, NiO with exposed {111} planes had a high Ni^{3+}/Ni^{2+} ratio, which was favorable for electron transport. Combining with these advantages, the NiO gas sensor with an exposed {111} surface could detect ethanol as low as 20 ppm (response value was 1.57).

In conclusion, the morphology has a significant impact on the ethanol-sensitive performance of NiO. The morphology with large specific surface area and high porosity facilitates the adsorption and transport of gas molecules. The special advantages of the hollow structure are beneficial to the detection of ethanol gas by NiO. Meanwhile, there are a still few reports on NiO with exposed {111} facets. Therefore, the synthesis of porous hollow nanofibers and hollow spheres, as well as NiO sensors with exposed {111} planes, can be considered in future topography work. Table 1 summarizes gas performance of NiO in different morphology. However, the effect of morphology adjustment on gas response is still weak and needs to be combined with other modification methods.

3. Cation Doping

Doping is an essential way to enhance performance. Whether it is adding metal elements to alloys to improve their mechanical properties or adding donor and acceptor elements to dielectric ceramics to improve dielectric properties, doping is very effective [80, 81]. Doping ions are divided into high-valence ions and low-valence ions, that is, the donor ions and acceptor ions mentioned above. In improving the ethanol sensing performance of NiO, ions with a higher valence state than Ni^{2+} are often introduced. It was found that the introduction of high-valence cations always enhanced the response by changing the ground-state resistance of NiO. As the high-valence ions replace the Ni^{2+} sites, those generate electrons to compensate for the substitution. At the same time, the extra electrons provided by the high-valence ions recombine with the holes in the NiO valence band. These two factors cause the hole concentration decrease in NiO and the ground-state resistance increase, resulting in an enhanced response to the target gas [82–84]. Furthermore, doping induces lattice distortion and introduces more oxygen vacancy defects. When detecting ethanol, ethanol molecules are easily trapped by oxygen vacancy defects, allowing more target molecules to react with NiO, resulting in a larger gas response [85–87]. Shailja et al. [88] introduced Ga^{3+} into NiO. The introduction of

Table 1: Gas performance of NiO in different morphology.

Material	Morphology	Conc. (ppm)	Operating temp (°C)	Response	Response/recovery time (s/s)	LOD (ppm)	References
NiO	Nanosheets	100	130	68.1%	5/20	0.2	[53]
NiO	Nanosheets	80	300	1.51	-/-	—	[52]
NiO	Nanosheets	50	240	11.15	4/7	1	[51]
NiO	Nanoflower	200	300	25	1.7/2.2	—	[55]
NiO	Nanoflower	200	300	55	4.8/7	—	[55]
NiO	Nanoflower	150	200	35	3/6	2.6	[56]
NiO	Nanoflower	100	190	46	-/-	—	[58]
NiO	Hollow sphere	800	240	3.1	-/-	—	[73]

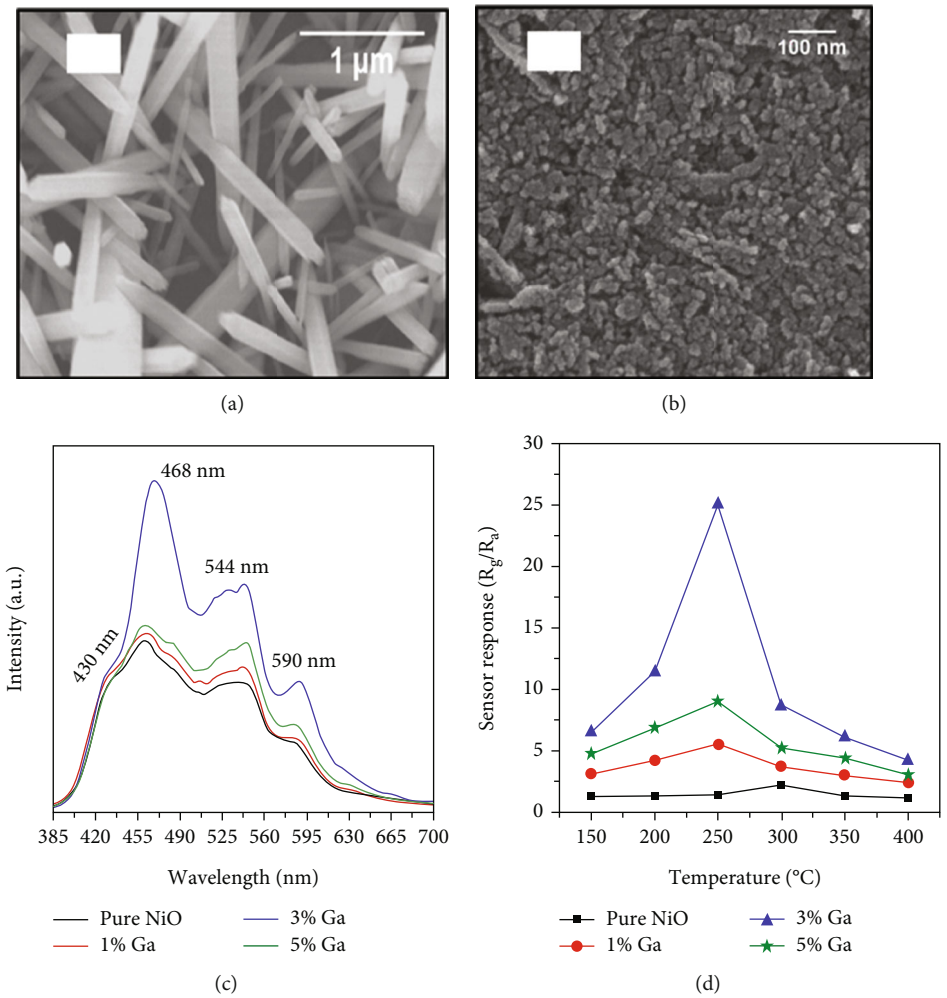

Figure 3: The SEM of (a) pure NiO and (b) Ga-NiO. (c) PL spectra of pure and Ga-doped NiO. (d) Gas response of pure NiO and Ga-NiO at various temperatures (reprinted/adapted by [88]).

Ga^{3+} transformed the structure of NiO from rod to a particle (Figures 3(a) and 3(b)). The BET test showed that this morphological transformation gave Ga-NiO a higher specific surface area (135.72 m^2/g). The intensity of the photoluminescence peaks of pure NiO was lower than that of Ga-NiO (Figure 3(c)), which meant that the introduction of Ga brought more defects to NiO. The sensor was tested for its ethanol-sensitive properties, and it was found that Ga-NiO had lower operating temperature and higher gas response (300°C for pure NiO and 250°C for Ga-NiO, respectively) (Figure 3(d)). When the Ga doping level was 3%, the gas response to 50 ppm ethanol at 250°C was 25, and the response/recovery time was 8/13 s. In addition, Ga-NiO could detect ethanol down to 10 ppm.

Mahmood et al. [89] studied the gas sensing performance of mesoporous Al-doped NiO ultralong nanowires to ethanol. Al^{3+} made NiO nanowires generate many pores, which

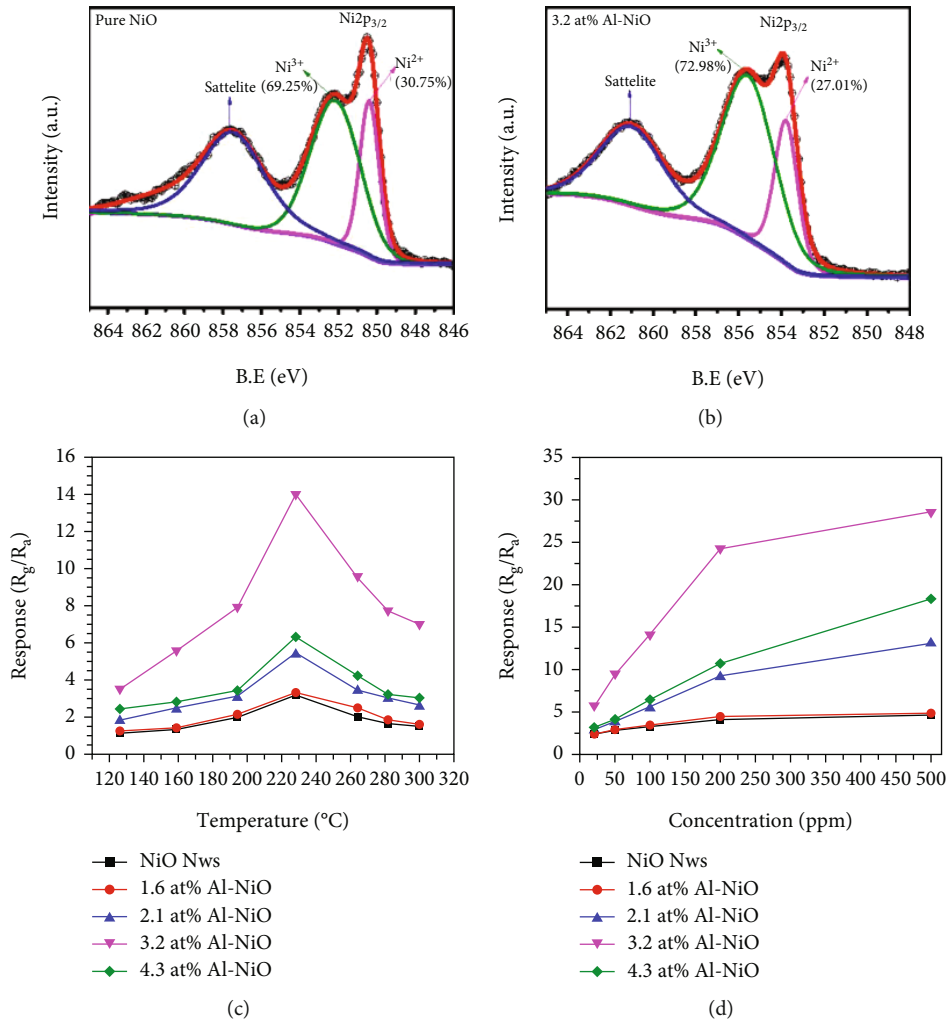

FIGURE 4: XPS spectra for Ni-2p3/2 of (a) pristine NiO and (b) 3.2 at% Al-doped NiO. (c) Gas response of pure NiO and Al-NiO at various temperatures. (d) Gas response of pure NiO and Al-NiO at 228°C under the ethanol vary from 10 ppm to 500 ppm (reprinted/adapted by [89]).

brought a larger specific surface area. Owing to the smaller atomic radius of Al^{3+} (0.54 Å for Al^{3+} and 0.69 Å for Ni^{2+}), Al^{3+} was easily substituted by Ni^{2+}, resulting in a greatly increased Ni^{3+}/Ni^{2+} ratio (Figures 4(a) and 4(b)). Larger Ni^{3+}/Ni^{2+} meant higher electronic performance, leading to better gas sensing performance. At 228°C, the sensitivity efficiency of 3.2 at% Al-NiO to 100 ppm ethanol showed 14.01, which was higher than that of undoped NiO (Figures 4(c) and 4(d)). Meanwhile, 3.2 at% Al-NiO enabled rapid detection of ethanol (response/recovery time of 73/76 s). For the enhanced sensitive performance, the authors believed that it was related to the changes in pores, oxygen species content, and carrier concentration brought about by the incorporation of Al^{3+}.

Besides doping high-valence ions, Chen et al. [90] also introduced Li^+ and Zn^{2+} into NiO. The study found that the incorporation of low-valence ions Li^+ and equivalent ions Zn^{2+} accelerated the detection of ethanol molecules by NiO. The response times of Li-NiO and Zn-NiO were 11 s and 17 s, respectively, while the response time of pure NiO was 33 s. However, Zn^{2+} hardly improved the response to ethanol, and Li^+ even degraded the sensitivity of NiO. The authors believed that the Li^+ extracted electrons from the valence band after forming the Li-O bond, leading the original resistance to decrease. Zn^{2+} in the same valence state hardly influenced the hole concentration, but the radius of Zn^{2+} was quite different from that of Ni^{2+}, so more defects were induced, which led to a slight improvement in the response of Zn^{2+} to ethanol.

The ethanol gas sensing performance of NiO will be worsened by doping low-valence Li^+ alone. But there was a study reported that the gas sensing performance of NiO may be ameliorated by adding high-valence ions at the same time as adding low-valence ions. Chang et al. [91] reported the simultaneous incorporation of Sc^{3+} and Li^+ into NiO nanoflowers. In addition to resulting in higher specific surface area, codoping could stabilize metastable surface oxygen vacancies (O_V) in metal oxides due to Li^+ active sites, so Sc and Li codoping increased the O_V ratio. Besides, Li^+ could make the bonding strength of surface oxygen weak, thereby promoting the surface redox reaction. When the doping

Table 2: Gas performance of doping NiO.

Material	Conc. (ppm)	Operating temp (°C)	Response	Response/recovery time (s/s)	LOD (ppb)	References
Ga-NiO	50	250	25	8/13	—	[88]
Al-NiO	100	228	14	73/76	—	[89]
Sc/Li-NiO	100	200	118.4	86/31	100	[91]
Fe-NiO	50	240	3.9	7/8	200	[92]
Mg-NiO	100	325	10.4	13/19	—	[93]

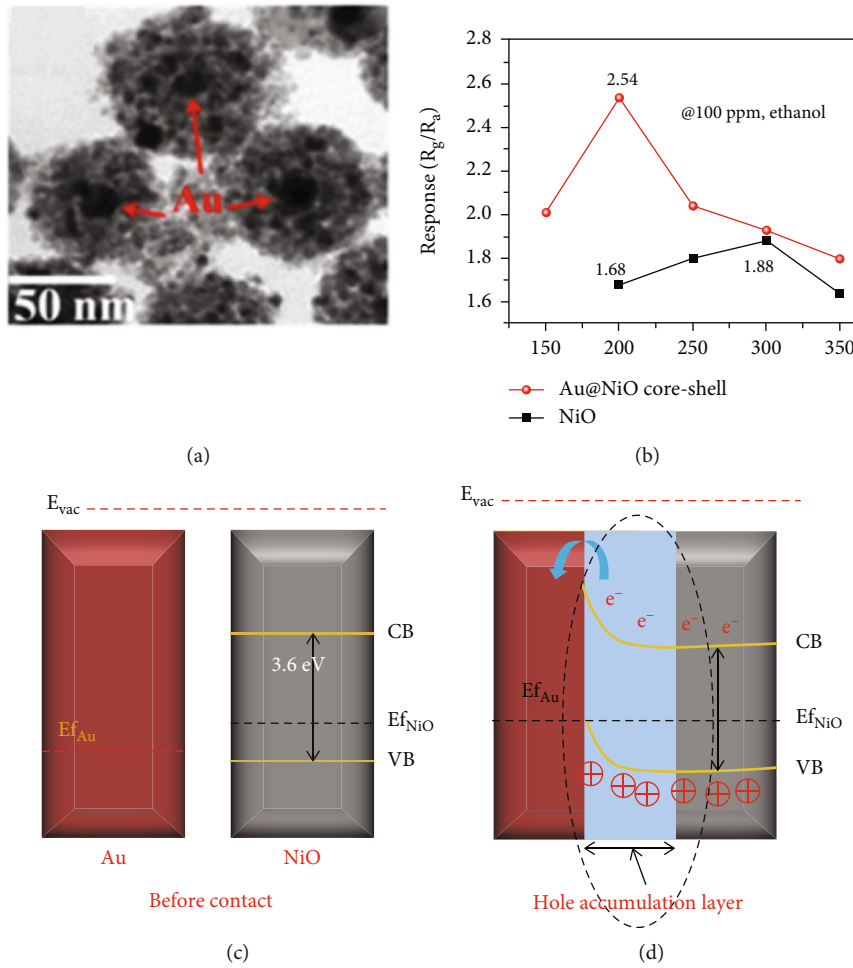

Figure 5: (a) The SEM of Au-NiO. (b) Gas response of NiO and Au-NiO at various temperatures. (c and d) The energy band diagram of Au-NiO before and after contact (reprinted/adapted by [95]).

amount was 2 at.% Sc and 5 at.% Li, the sensitivity to 100 ppm ethanol at 200°C was 118.4, which was 105 times higher than that of pristine NiO. Meanwhile, the response time and recovery time of the Sc/Li-NiO sensor were 86 s and 31 s. The LOD was as low as 10 ppb. According to defect characterization and first-principle calculations, the codoping of Sc^{3+} and Li^+ significantly increased the stable O_V and Ni^{3+}, which greatly promoted the adsorption of ethanol molecules, resulting in an excellent gas response.

In this section, we discussed the mechanism by which cation doping enhances the performance of NiO gas sensors. NiO is mainly doped with high-valence cations, and the changes in hole concentration and defect concentration caused by high-valence cations make NiO have better ethanol sensing performance. In particular, low-valence cations do not seem to be a method to enhance the sensitive performance of NiO. However, by doping with high-valence ions and low-valence ions, the unique properties of low-valence ions can be exerted, while high-valence ions improve the sensitivity. In the future, for the development of doping methods, we can pay more attention to high-valence/low-valence codoping. Table 2 exhibits gas performance of NiO doping by metal cation. However, the amount of ion doping is less controllable, and whether the ions successfully enter the lattice is difficult to control, while doping noble metal particles is relatively easy to control.

Table 3: Gas performance of NiO functional by precious metal particles.

Material	Conc. (ppm)	Operating temp (°C)	Response	Response/recovery time (s/s)	References
Au-NiO	100	200	2.54	250/420	[95]
Au-NiO	1000	325	442%	-/-	[97]
Pt-NiO	100	200	20.85	-/-	[96]

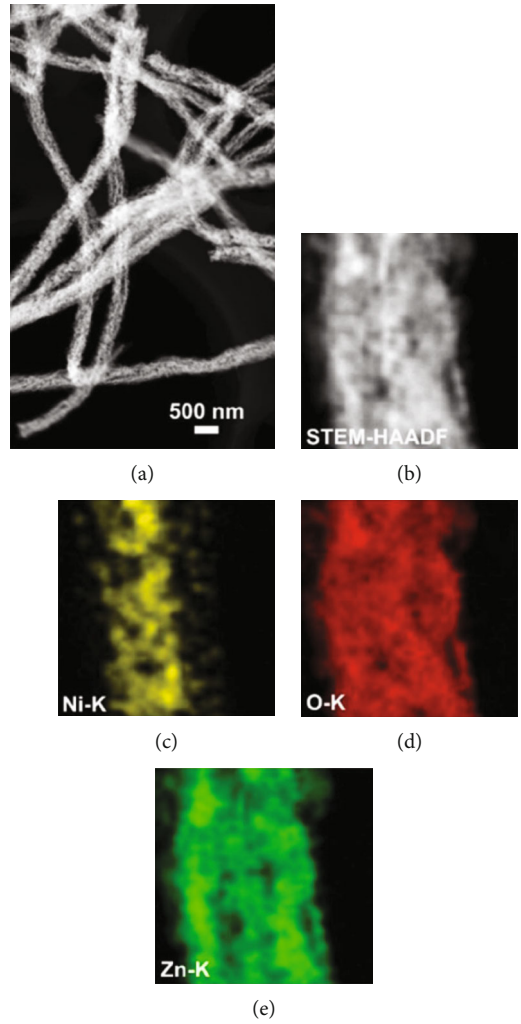

Figure 6: (a) TEM of NiO-ZnO. (b) HAADF-STEM image of NiO-ZnO. Elemental mapping images of (c) Ni, (d) O, and (e) Zn (reprinted/adapted by [108]).

4. Precious Metal Particle Loading

Precious metal particle loading is a common way to improve sensitive properties. The improved performance of precious metal particles can be attributed to two reasons. First is chemical sensitization. Chemical sensitization exploits the catalytic properties of precious metal particles. Noble metal particles can catalyze O_2 molecules to capture electrons from the valence band of NiO and dissociated into ionic species, resulting in more holes in the valence band [94]. A lower baseline resistance can result in a larger change in resistance, meaning better sensitivity. This results in a higher sensing response to ethanol gas. Second is electron sensitization. Electron sensitization utilizes a change in the Fermi level. After the precious metal particles are in contact with NiO, the Fermi levels of the two are not at the same level. To reach electronic equilibrium, the Fermi level of NiO will shift, creating additional depletion layers and reducing the HAL thickness [68].

Enhanced sensitive properties are usually caused by a combination of the two. For example, Majhi et al. [95] utilized the electronic and chemical sensitization effects of Au to obtain an Au-NiO gas sensor with excellent gas sensing performance. Au particles were encapsulated inside NiO to form a core-shell structure (Figure 5(a)). The optimal operating temperature of Au-NiO was 200°C, which was 100°C lower than that of NiO (Figure 5(b)). Au-NiO obtained a 2.54 response to 100 ppm

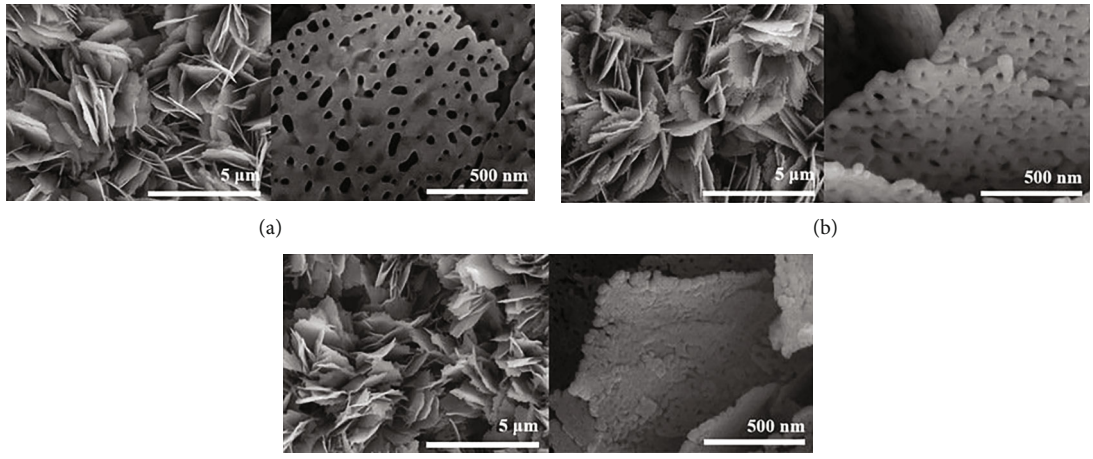

Figure 7: SEM of NiO/ZnO with different sputtering times [63] (open access).

ethanol at 200°C, and the response time and recovery time were 250 s and 420 s. Compared with pristine NiO, Au-NiO had a larger response and more rapid response/recovery speed. Since the Fermi levels of Au and NiO were not at the same level, Au and NiO contacted to form a Schottky junction (Figures 5(c) and 5(d)). At the same time, additional HAL was formed near the Au-NiO interface, which increased the quantity of holes in Au-NiO, resulting in a larger resistance. Fu et al. [96] synthesized Pt-NiO nanotubes by electrospinning, and the NiO nanotubes functionalized by Pt were dendriform. Due to the activation and catalytic effect of Pt on NiO, the response of 0.7% Pt-NiO nanotubes at 100 ppm ethanol and 200°C was 20.85, while pure NiO got 2.06 under the equal environment. Park et al. [97] studied the sensing performance of pristine NiO and Au-modified NiO for ethanol. The responses of NiO and Au-NiO sensors to 1000 ppm ethanol at 325°C were 273% and 442%, respectively. The author attributed the enhanced sensitive performance to the additional depletion layer and Schottky barrier formed by the Au particles, high catalytic activity, and smaller diameter of Au-NiO.

Although the chemical catalysis and electronic catalysis of precious metal particles bring excellent ethanol sensing properties to NiO, there are few reports on the modification of NiO by those in recent years. The main reason is that precious metal particles are expensive. Considering the cost, it is difficult to apply them to actual production. Table 3 is gas performance of NiO functional by precious metal particles in recent years. The Schottky barrier generated by the combination of noble metal particles and NiO is similar to PN heterojunctions, so scholars are keen to form heterojunctions to improve the ethanol-sensitive properties of NiO.

5. Composites

NiO, p-type semiconductor, is often combined with n-type semiconductors to form a PN heterojunction. The Fermi level of the p-type semiconductor is lower than that of the n-type semiconductor. When the two are in contact, electrons move to the p-type semiconductor and holes move to the n-type semiconductor, resulting in band bending. An EDL is then formed in the hetero area and strongly inhibits the conduction channel. When the heterojunction contacts the target gas, electron release greatly reduces the potential barrier at the heterojunction, causing a bigger change in resistivity and a higher sensitivity [46, 98, 99].

5.1. Metal Oxides. In recent years, NiO has been reported to recombine with n-type semiconductors such as ZnO [63, 100–110], SnO_2 [67, 111–118], WO_3 [119–121], Fe_2O_3 [122–124], and In_2O_3 [125, 126].

The n-type semiconductor ZnO has received attention due to its low cost and fast response speed, which can detect a variety of gases [17, 18, 127]. Among the recent reports, NiO- and ZnO-combined sensors have the most detection of ethanol. Bai et al. [108] used electrospinning and atomic layer deposition (ALD) to design a NiO/ZnO core-shell nanotube (CSNT), in which NiO was the core and ZnO was the shell (Figure 6). There were many pores and some hollow structures in such nanotubes, which helped gas molecules to be fixed in the pore channels. NiO/ZnO CSNTs obtained a gas response of 16 for the detection of 100 ppm ethanol at 325°C, and it was much bigger than that of pristine ZnO (8.8) and pure NiO (2.5). In addition, NiO/ZnO had a shorter response time (13 s) but a longer recovery time (498 s). The nice gas sensing performance thanked to the shell thickness of NiO/ZnO close to the Debye length (λD). In this case, a fully electron-depleted state was established and the most effective resistance modulation occurred, causing the highest gas sensing performance of NiO/ZnO. When the shell of the core-shell structure was thicker, the resistance modulation through the shell would be significantly reduced, owing to the depletion of some electron in the thick shell, thus resulting in a reduced gas response. Liang et al.'s team [63] sputter-deposited NiO onto porous ZnO nanosheets. NiO was uniformly attached to ZnO, and the addition of NiO narrowed the pore size on ZnO nanosheets (Figure 7). Due to the different work functions, a built-in electric field was formed at the NiO/ZnO heterojunction interface, which also induced band bending. The formation of the built-in electric field leads to a higher barrier height and a higher initial resistance. After exposure to ethanol

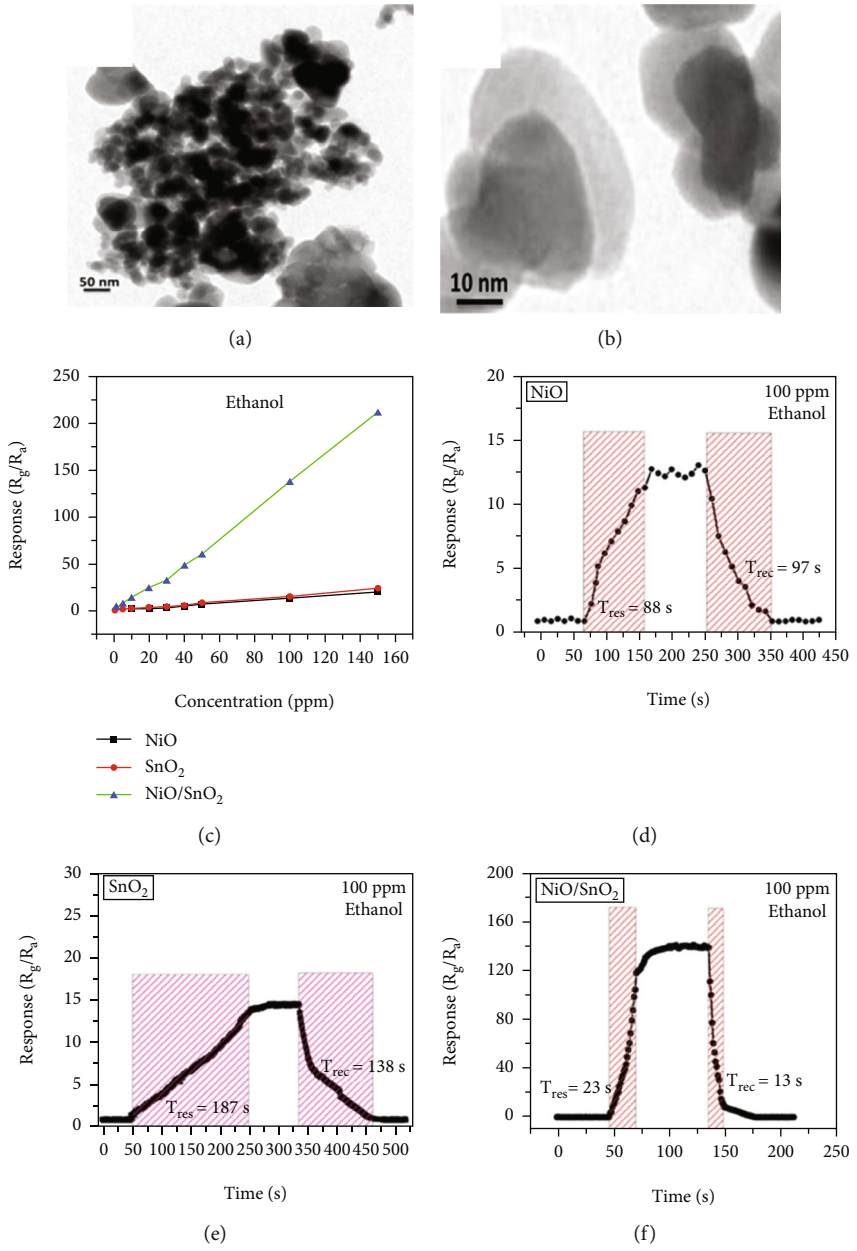

Figure 8: (a and b) HRTEM of NiO/SnO_2. (c) Gas response of NiO, SnO_2, and NiO/SnO_2 under various ethanol concentrations. Response and recovery curves of (d) NiO, (e) SnO2, and (f) NiO/SnO_2 (reprinted/adapted by [111]).

gas, electrons were released, reducing the barrier height of the depletion layer. Besides, NiO/ZnO had a distinctive porous nanosheet structure, which provided abundant surface active sites and a lot of gas diffusion channels for ethanol molecules.

There have been many reports that SnO_2 is easily composited with other materials to form heterostructures, which is a perfect sensitive material and is often used in ethanol gas sensors [13, 15, 128]. Jayababu et al. [111] composited NiO with SnO_2 to form an ethanol sensor. NiO had a semi-shielding effect on SnO_2 nanoparticles by HRTEM; that is, NiO partially covered SnO_2 (as shown in Figures 8(a) and 8(b)). Due to the PN heterostructure and catalytic activity brought by NiO, the NiO/SnO_2 sensors exhibited excellent sensing performance for ethanol. At RT, NiO/SnO_2 achieved a response as high as 140 for ethanol, much higher than SnO_2 and NiO (seen in Figure 8(c)). Beyond that, NiO/SnO_2 showed fast response and recovery speed, with response and recovery times of 23 s and 13 s, respectively (as shown in Figures 8(d)–8(f)). Zhang et al.'s group [115] synthesized a novel NiO/SnO_2 vertical nanotube composite film, which consisted of 20 nm diameter NiO nanosheets attached to one-dimensional SnO_2 nanotubes (Figures 9(a) and 9(b)). When the molar ratio of Ni^{2+}/Sn^{4+} was 5%, NiO/SnO_2 had high adsorbed oxygen. At 250°C, it had the highest gas response to ethanol (123.7 for 1000 ppm ethanol, as shown in Figure 9(c)). Figure 9(d) is the gas response curve for five gases. NiO/SnO_2 has high selectivity for ethanol, which was beneficial to realize the efficient detection of ethanol. Since

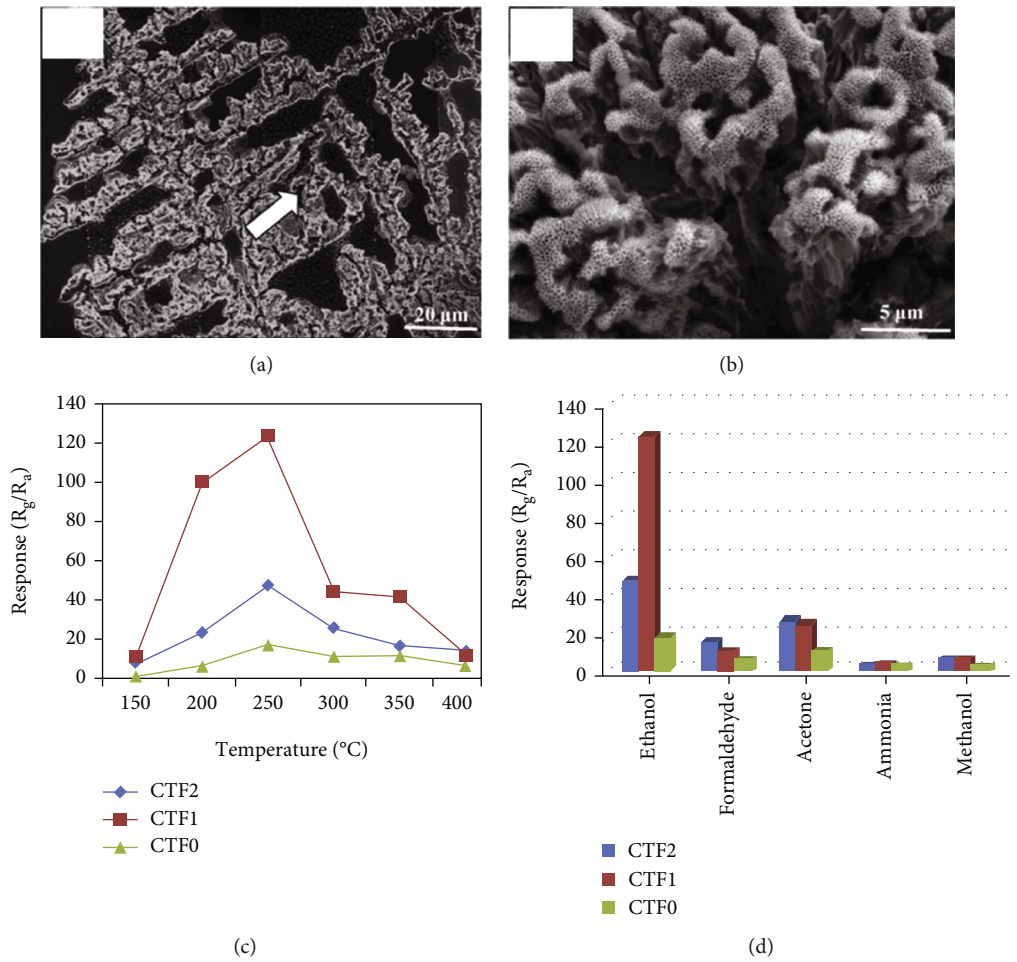

Figure 9: (a) SEM of NiO/SnO_2. (b) Enlarged image of (a) where the white arrow points. (c) Gas response of NiO/SnO_2 under different temperatures. (d) Gas response of NiO/SnO_2 under different gases (reprinted/adapted by [115]).

SnO_2 nanotubes could transport electrons quickly, NiO/SnO_2 could rapidly detect ethanol compounds within 10 s. After the heterojunction of SnO_2 and NiO was formed, the band bending led to the narrowing of the electron transport channel, which increased the ground-state resistance. The higher ground-state resistance was beneficial in enhancing the gas sensing performance, so the respond value of NiO/SnO_2 was higher than NiO.

α-Fe_2O_3, a n-type semiconductor, has been demonstrated as an ethanol sensor due to its low cost, high stability, and environmental friendliness [129–131]. Tan et al. [124] employed microwave-assisted liquid-phase synthesis to support Fe_2O_3 on NiO nanosheets. Owing to the enhanced sensitivity of the heterojunction pair of Fe_2O_3 and NiO, the 1.5% Fe_2O_3/NiO sensor got a high response of 170.7 and an ultrafast response/recovery speed (0.5/14.6 s) to 100 ppm ethanol. In_2O_3 has received attention in gas sensors because of its stable electrical conductivity, good chemical stability, and low cost [28, 132]. Yan et al. [125] successfully synthesized In_2O_3/NiO composites through electrospinning technology and ion exchange reaction. The NiO nanosheets were arranged in one dimension, and the In_2O_3 nanoparticles were uniformly attached to them. During the detection of ethanol, the charge carriers of In_2O_3/NiO were conducted through the continuous NiO. The formation of the PN junction created a thicker hole depletion layer under In_2O_3. Therefore, a small change in carrier concentration resulted in a larger gas response. WO_3 is favored in ethanol gas sensors because of its special physicochemical and electrical properties [133, 134]. Juang and Wang's team [120] found that the composite of porous NiO spheres and WO_3 nanoplates had a response of 155% to ethanol, which was 1.4 times that of pure WO_3 nanoplates. The enhanced ethanol sensitivity was attributed to the formation of the PN heterojunction. Table 4 shows gas performance of NiO/metal oxide-based composites.

5.2. Bimetallic Oxides. Apart from the above single metal oxides, bimetallic oxides have also been used to improve NiO materials. $LaFeO_3$ has been studied in gas sensors owing to its high electrical conductivity and good redox properties [136, 137]. Hao et al.'s team [138] modified NiO nanosheets onto porous $LaFeO_3$ microspheres and studied their ethanol sensing properties. Figures 10(a) and 10(b) are the SEM images of $LaFeO_3$ and $NiO/LaFeO_3$. The surface of $LaFeO_3$ had abundant pore structure, and NiO nanosheets were uniformly distributed on the $LaFeO_3$ microspheres. This morphology effectively increased the contact area between the composite and ethanol. Figure 10(c) is the gas response of $NiO/LaFeO_3$ and $LaFeO_3$ under different temperatures at 10 ppm ethanol. The optimum

Table 4: Gas performance of NiO/metal oxide-based composites.

Material	Conc. (ppm)	Operating temp (°C)	Response	Response/recovery time (s/s)	LOD (ppm)	References
NiO/SnO_2	100	160	13.4	-/-	—	[112]
NiO/SnO_2	100	RT	140	23/13	1	[111]
NiO/SnO_2	100	160	23.87	57/66	—	[113]
NiO/SnO_2	50	300	9	-/-	5	[114]
NiO/SnO_2	1000	250	123.7	10/58	—	[115]
NiO/SnO_2	1000	150	84.7	5/15	—	[116]
NiO/SnO_2	100	260	153	-/-	5	[117]
NiO/SnO_2	1000	320	576.5	9/34	—	[118]
NiO/SnO_2	100	75	248	-/-	—	[67]
NiO/ZnO	100	260	61	-/-	—	[101]
NiO/ZnO	100	200	11.3	4/78	—	[63]
NiO/ZnO	100	350	54	-/-	—	[102]
NiO/ZnO	200	300	33	-/-	—	[103]
NiO/ZnO	250	RT	32.48%	2.7/3.6	—	[105]
NiO/ZnO	500	400	37.5	2.1/4.1	—	[106]
NiO/ZnO	100	325	16	13/498	—	[108]
NiO/ZnO	20	200	49	4/28	3	[110]
NiO/WO_3	100	300	58.2	-/-	—	[119]
NiO/WO_3	200	175	155%	19/20	—	[120]
NiO/WO_3	200	320	10	-/-	—	[121]
NiO/Fe_2O_3	100	255	170.7	0.5/14.6	0.2	[124]
NiO/In_2O_3	100	280	4.61	-/27	—	[125]
NiO/In_2O_3	5	350	9.76	-/23	2	[126]
NiO/Co_2O_3	100	250	4.26	-/-	0.073	[135]

operating temperature of $NiO/LaFeO_3$ was 240°C, while $LaFeO_3$ was 260°C. It meant that $NiO/LaFeO_3$ could lower the operating temperature, which was beneficial for low temperature sensing. The response recovery curves of 10 ppm ethanol at 240°C are shown in Figure 10(d). Both $NiO/LaFeO_3$ and $LaFeO_3$ had good reproducibility, and the response of $NiO/LaFeO_3$ was much higher than that of $LaFeO_3$. In addition, $NiO/LaFeO_3$ had fast response and recovery speed (response time and recovery time were 2 s and 9 s, respectively). The response of $NiO/LaFeO_3$ also increased with increasing ethanol concentration and was consistently higher than that of pristine $LaFeO_3$ (Figure 10(e)). The $NiO/LaFeO_3$-based sensors detected five different gases, as shown in Figure 10(f). The $NiO/LaFeO_3$ sensors exhibited a good selectivity to ethanol, which provided a new way to fabricate high-performance ethanol sensors. The enhanced sensing performance was ascribed to the special structure, the catalytic performance of NiO, and the electronic modulation of the Fermi level.

Haq et al. [139] used a hydrothermal method to decorate NiO nanoparticles on $ZnSnO_3$ fibers (Figure 11(a)). The gas responses of all samples at different temperatures were volcanic shape (Figure 11(b)). It was worth noting that $NiO/ZnSnO_3$ obtained the highest response at 160°C, while NiO obtained the highest response at 200°C. It meant that $NiO/ZnSnO_3$ obtained the highest response at 160°C. The $ZnSnO_3$ composite could detect ethanol at lower temperatures. As in Figure 11(c), ethanol, acetone, toluene, xylene, and benzene were detected. The $NiO/ZnSnO_3$ sensors possessed a much higher response to ethanol than other gases, with better selectivity. Figure 11(d) is the gas response of $NiO/ZnSnO_3$, NiO, and $ZnSnO_3$ to different ethanol concentrations at 160°C. As the ethanol concentration increased, the gas response also increased gradually. And $NiO/ZnSnO_3$ obtained the best ethanol sensing performance. The response of $NiO/ZnSnO_3$ to 20 ppm ethanol gas at 160°C was 23.95. The enhanced sensitivity was attributed to the more oxygen content of $ZnSnO_3$ after NiO decoration. At the same time, $ZnSnO_3$ was an n-type semiconductor. The modulation effect brought by the PN heterojunction also made the resistance change of $NiO/ZnSnO_3$ larger, resulting in a higher gas response. Table 5 shows gas performance of NiO/bimetallic oxide-based composites.

In this section, we discussed the reported composites of NiO combined with MOS such as ZnO, SnO_2, Fe_2O_3, In_2O_3, WO_3, and bimetallic oxides $LaFeO_3$ and ZnSnO3 in ethanol sensing. The combination of NiO with these oxides mainly relies on the electronic modulation brought about by the formation of PN heterojunctions. Although NiO composites have been reported, most of them are about oxides. For the future, other potential gas sensing materials, such as conducting polymers, MXene, and carbon-based materials, can also be compounded with NiO to improve the sensitive properties.

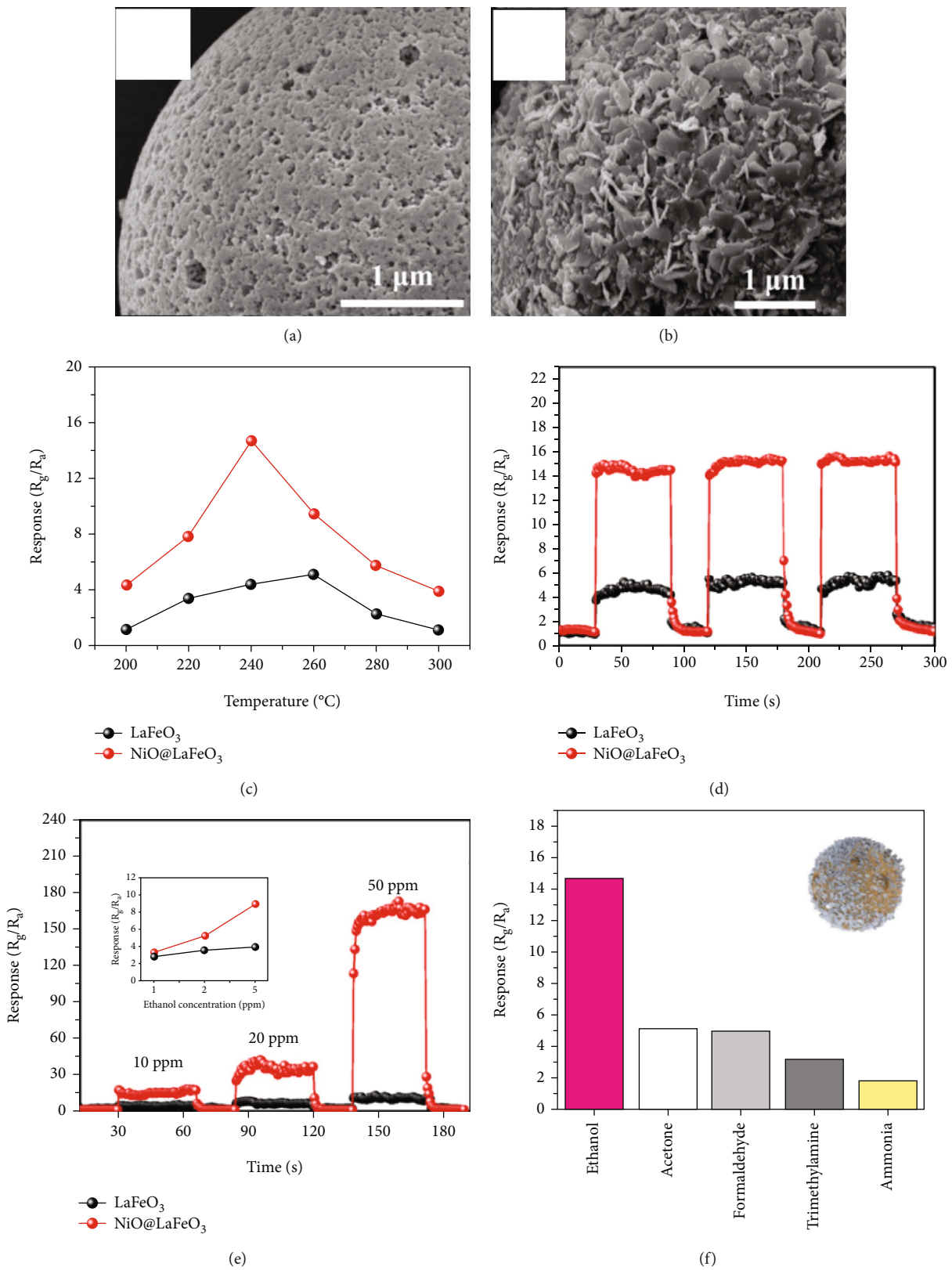

Figure 10: (a) SEM of $LaFeO_3$. (b) SEM of $NiO/LaFeO_3$. (c) Gas response of $NiO/LaFeO_3$ and $LaFeO_3$ under different temperatures at 10 ppm ethanol. (d) Response and recovery curves of $NiO/LaFeO_3$ and $LaFeO_3$ at 10 ppm ethanol. (e) Dynamic response curves of $NiO/LaFeO_3$ and $LaFeO_3$ to different ethanol concentrations at 240°C. (f) Gas response of $NiO/LaFeO_3$ under 10 ppm different gases (reprinted/adapted by [138]).

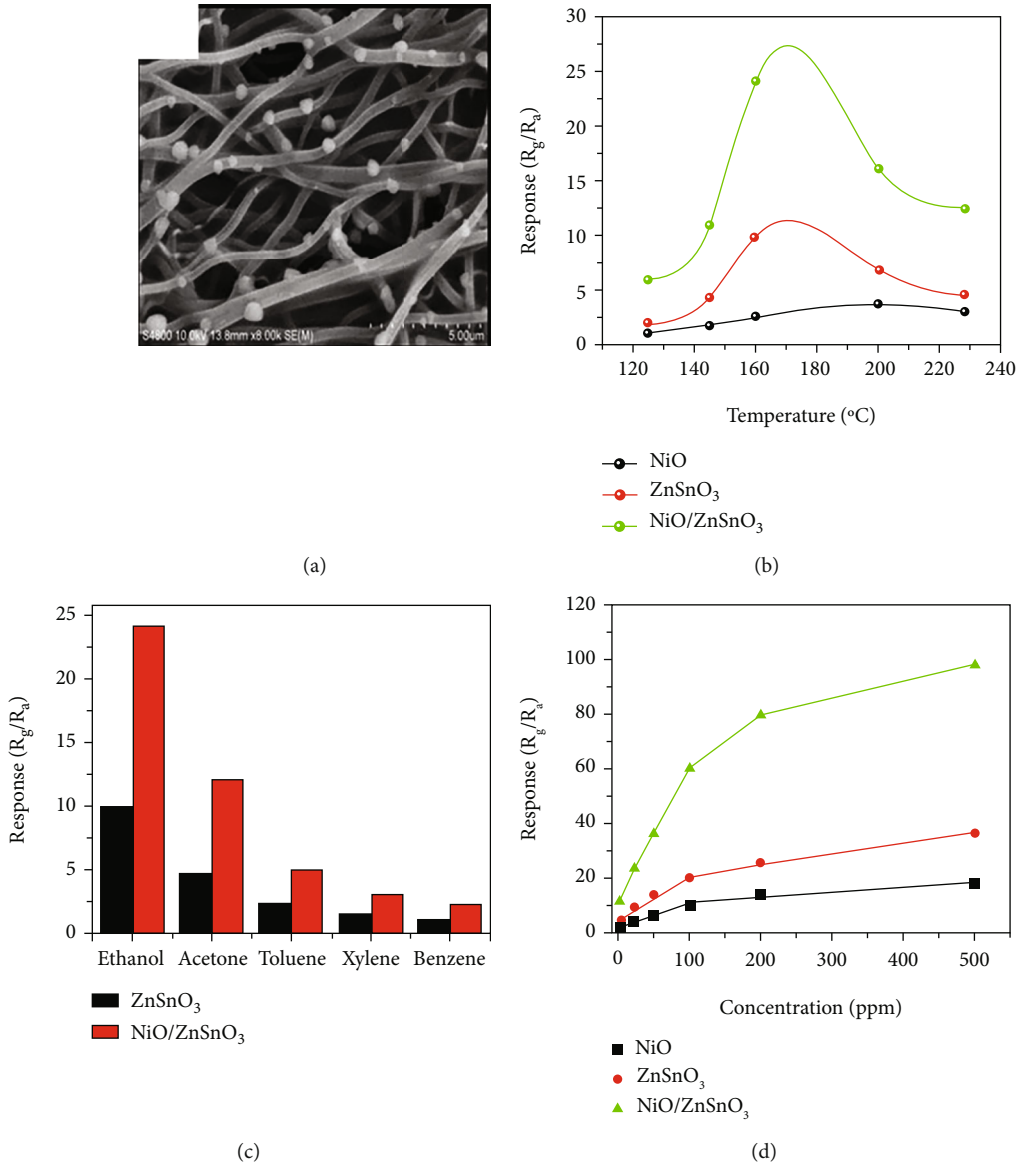

Figure 11: (a) SEM of $NiO/ZnSnO_3$. (b) Gas response of $NiO/ZnSnO_3$, NiO, and $ZnSnO_3$ under different temperatures at 20 ppm ethanol. (c) Gas response of $NiO/ZnSnO_3$ and $ZnSnO_3$ under 20 ppm different gases. (d) Gas response of $NiO/ZnSnO_3$, NiO, and $ZnSnO_3$ to different ethanol concentrations at 160°C (reprinted/adapted by [139]).

Table 5: Gas performance of NiO/bimetallic oxide-based composites.

Material	Conc. (ppm)	Operating temp (°C)	Response	Response/recovery time (s/s)	LOD (ppm)	References
$NiO/LaFeO_3$	10	240	—	2/9	—	[138]
$NiO/ZnSnO_3$	20	160	23.95	-/-		[139]

6. Outlook

Although there have been many reports on the ethanol-sensitive performance of NiO in recent years, reports on the in-depth study of the selective mechanism of ethanol are still rare. Most of the literature addresses the fact that there is selectivity but does not discuss the ultimate mechanism of selectivity. Highly selective gas sensors are necessary in complex gas environments, where they need to accurately identify target gases among interfering gases. The study of the mechanism of selectivity is helpful for the further development of highly selective gas sensors. In future work, researchers can further study the mechanism of ethanol selectivity to facilitate the efficient detection of ethanol in environments with interfering gases. At the same time, molecular imprinting technology is expected to be applied to improve selectivity. Molecular

imprinting is a lock-and-key technology that enables specific identification of specific gases. Combining molecular imprinting technology with resistive sensors is believed to further address the selectivity challenges of gas sensors.

7. Conclusion

In conclusion, this review presented an overview of NiO-based ethanol gas sensors. We first introduced the effect of modified NiO morphology on ethanol performance that has been reported in recent years. The morphology with large specific surface area and high porosity was considered to be the structure that can bring high gas response. Then, we discussed the enhanced effect of the doping of metal cations and precious metal particle loading on the ethanol-sensitive properties of NiO. Doping ions increased the ground-state resistance and increased the oxygen defect concentration of NiO. The effects of precious metal particles on the performance of NiO included chemical sensitization and electronic sensitization. Finally, the related contents of NiO forming composites with metal oxides and bimetallic oxides were discussed. In this section, the specific improvement mechanism was discussed first, and then, the related work of researchers in recent years was summarized.

Data Availability

All data can be obtained from corresponding author Yanqiong Li.

Conflicts of Interest

The authors declare that they have no conflicts of interest.

Acknowledgments

This work was supported by the Graduate Research and Innovation Foundation of Chongqing, China (Grant No. CYS22003).

References

[1] S. Singh, J. Deb, S. Kumar, U. Sarkar, and S. Sharma, "Selective N,N-dimethylformamide vapor sensing using MoSe2/multiwalled carbon nanotube composites at room temperature," *Acs Applied Nano Materials*, vol. 5, no. 3, pp. 3913–3924, 2022.

[2] W. Qin, R. Zhang, Z. Yuan, C. Xing, and F. Meng, "Preparation of p-$LaFeO_3$/n-Fe_2O_3 heterojunction composites by one-step hydrothermal method and gas sensing properties for acetone," *Ieee Transactions on Instrumentation and Measurement*, vol. 71, pp. 1–9, 2022.

[3] B. Huang, W. Zeng, and Y. Li, "Synthesis of ZnO@ZIF-8 nanorods with enhanced response to VOCs," *Journal of the Electrochemical Society*, vol. 169, no. 4, p. 047508, 2022.

[4] J. Fang, Z.-H. Ma, J.-J. Xue, X. Chen, R.-P. Xiao, and J.-M. Song, "Au doped In_2O_3 nanoparticles: preparation, and their ethanol detection with high performance," *Materials Science in Semiconductor Processing*, vol. 146, p. 106701, 2022.

[5] S. K. Rao, A. K. Priya, S. M. Kamath et al., "Unraveling the potential of Gd doping on mullite $Bi_2Fe_4O_9$ for fiber optic ethanol gas detection at room temperature," *Materials Chemistry and Physics*, vol. 278, p. 125646, 2022.

[6] A. Akhtar, S. Sadaf, J. Liu et al., "Hydrothermally synthesized spherical g-C_3N_4-$NiCo_2O_4$ nanocomposites for ppb level ethanol detection," *Journal of Alloys and Compounds*, vol. 911, p. 165048, 2022.

[7] B. Du, Y. Zheng, J. Ye, D. Wang, C. Mao, and N. Sun, "Photoluminescence-based sensing of ethanol gas with ultrafine WO_3 nanorods," *Optics Letters*, vol. 47, no. 5, pp. 1145–1148, 2022.

[8] P. Biswas, C. Zhang, Y. Chen et al., "A portable micro-gas chromatography with integrated photonic crystal slab sensors on chip," *Biosensors-Basel*, vol. 11, no. 9, p. 326, 2021.

[9] M. B. Banerjee, S. R. Chowdhury, R. B. Roy et al., "Development of a low-cost portable gas sensing system based on molecularly imprinted quartz crystal microbalance sensor for detection of eugenol in clove oil," *Ieee Transactions on Instrumentation and Measurement*, vol. 70, pp. 1–10, 2021.

[10] W. Qin, Z. Yuan, H. Gao, R. Zhang, and F. Meng, "Perovskite-structured $LaCoO_3$ modified ZnO gas sensor and investigation on its gas sensing mechanism by first principle," *Sensors and Actuators B-Chemical*, vol. 341, p. 130015, 2021.

[11] K. Zhang, S. Qin, P. Tang, Y. Feng, and D. Li, "Ultra-sensitive ethanol gas sensors based on nanosheet-assembled hierarchical ZnO-In_2O_3 heterostructures," *Journal of Hazardous Materials*, vol. 391, p. 122191, 2020.

[12] J. van den Broek, S. Abegg, S. E. Pratsinis, and A. T. Guentner, "Highly selective detection of methanol over ethanol by a handheld gas sensor," *Nature Communications*, vol. 10, no. 1, 2019.

[13] P. Wang, T. Song, G. Gao, K. Matras-Postolek, and P. Yang, "SnO_2 clusters embedded in TiO_2 nanosheets: heterostructures and gas sensing performance," *Sensors and Actuators B-Chemical*, vol. 357, p. 131433, 2022.

[14] E. P. Nascimento, R. N. Araujo, H. C. T. Firmino et al., "Parallel-solution blow spun Al-SnO_2/F-SnO_2 fibers as an efficient room temperature ethanol sensor," *Ceramics International*, vol. 48, no. 9, pp. 13163–13174, 2022.

[15] X. Tian, H. Cao, H. Wang, J. Wang, X. Wei, and X. Wu, "Acid vapor oxidation growth of SnO_2 nanospheres with ultra-high sensitivity to ethanol detection at low temperature," *Journal of Alloys and Compounds*, vol. 905, p. 164229, 2022.

[16] B. Jiang, J. Lu, W. Han et al., "Hierarchical mesoporous zinc oxide microspheres for ethanol gas sensor," *Sensors and Actuators B-Chemical*, vol. 357, p. 131333, 2022.

[17] M. J. Ahemad, T. D. Le, D.-S. Kim, and Y.-T. Yu, "Bimetallic AgAualloy@ZnO core-shell nanoparticles for ultra-high detection of ethanol: potential impact of alloy composition on sensing performance," *Sensors and Actuators B-Chemical*, vol. 359, p. 131595, 2022.

[18] W. Photaram, M. Liangruksa, M. Aiempanakit et al., "Design and fabrication of zinc oxide-graphene nanocomposite for gas sensing applications," *Applied Surface Science*, vol. 595, p. 153510, 2022.

[19] R.-H. Wang, W. Wen, S. Zheng, Z. Ye, and J.-M. Wu, "Layered mesoporous SnO_2 for effective ethanol detection at reduced working temperature," *Sensors and Actuators B-Chemical*, vol. 362, p. 131805, 2022.

[20] M. Pfeiffer and C. Hess, "Application of transient infrared spectroscopy to investigate the role of gold in ethanol gas sensing over Au/SnO_2," *Journal of Physical Chemistry C*, vol. 126, no. 8, pp. 3980–3992, 2022.

[21] C. Wang, R. Li, L. Feng, and J. Xu, "The SnO_2/MXene composite ethanol sensor based on MEMS platform," *Chemosensors*, vol. 10, no. 3, p. 109, 2022.

[22] X. Li, C.-X. Liu, J.-R. Zhou, Y. Ma, and S.-P. Ruan, "Study on ethanol gas sensor based on hierarchical structured NiO/Zn_2SnO_4 nanoflowers," *Chinese Journal of Analytical Chemistry*, vol. 50, no. 4, pp. 564–573, 2022.

[23] Z. Shao, Z. Zhao, P. Chen et al., "Enhanced ethanol response of Ti3C2TXMXene derivative coupled with NiO nanodisk," *Inorganic and Nano-Metal Chemistry*, vol. 52, pp. 1–9, 2022.

[24] S. Singh and S. Sharma, "Temperature-based selective detection of hydrogen sulfide and ethanol with MoS_2/WO_3 composite," *Acs Omega*, vol. 7, no. 7, pp. 6075–6085, 2022.

[25] M. Tomic, Z. Fohlerova, I. Gracia, E. Figueras, C. Cane, and S. Vallejos, "UV-light activated APTES modified WO_{3-x} nanowires sensitive to ethanol and nitrogen dioxide," *Sensors and Actuators B-Chemical*, vol. 328, p. 129046, 2021.

[26] E. Spagnoli, S. Krik, B. Fabbri et al., "Development and characterization of WO_3 nanoflakes for selective ethanol sensing," *Sensors and Actuators B-Chemical*, vol. 347, p. 130593, 2021.

[27] X. Li, Y. Wang, P. Cheng et al., "High-performance ethanol sensor of wrinkled microspheres by spray pyrolysis," *Sensors and Actuators B-Chemical*, vol. 344, p. 130309, 2021.

[28] T.-T. Liang, D.-S. Kim, J.-W. Yoon, and Y.-T. Yu, "Rapid synthesis of rhombohedral In_2O_3 nanoparticles via a microwave-assisted hydrothermal pathway and their application for conductometric ethanol sensing," *Sensors and Actuators B-Chemical*, vol. 346, p. 130578, 2021.

[29] X. Jin, Y. Li, B. Zhang, X. Xu, G. Sun, and Y. Wang, "Temperature-dependent dual selectivity of hierarchical porous In_2O_3 nanospheres for sensing ethanol and TEA," *Sensors and Actuators B-Chemical*, vol. 330, p. 129271, 2021.

[30] K. Li, Y. Luo, B. Liu, H. Wang, L. Gao, and G. Duan, "Theory-guided oxygen-vacancy for enhancing H_2S sensing performance of NiO," *Chemical Engineering Journal*, vol. 432, p. 134302, 2022.

[31] M. Shoorangiz, L. Shariatifard, H. Roshan, and A. Mirzaei, "Hydrothermally synthesized flower-like vanadium oxide nanostructures for ethanol sensing studies," *Materials Science in Semiconductor Processing*, vol. 137, p. 106241, 2022.

[32] G. Yuan, Y. Zhong, Y. Chen, Q. Zhuo, and X. Sun, "Highly sensitive and fast-response ethanol sensing of porous Co_3O_4 hollow polyhedra via palladium reined spillover effect," *RSC Advances*, vol. 12, no. 11, pp. 6725–6731, 2022.

[33] P. T. Moseley, "Progress in the development of semiconducting metal oxide gas sensors: a review," *Measurement Science and Technology*, vol. 28, no. 8, p. 082001, 2017.

[34] N. Joshi, L. F. da Silva, H. Jadhav et al., "One-step approach for preparing ozone gas sensors based on hierarchical $NiCo_2O_4$ structures," *RSC Advances*, vol. 6, no. 95, pp. 92655–92662, 2016.

[35] N. Joshi, L. F. da Silva, H. S. Jadhav et al., "Yolk-shelled $ZnCo_2O_4$ microspheres: surface properties and gas sensing application," *Sensors and Actuators B-Chemical*, vol. 257, pp. 906–915, 2018.

[36] J. Yu, C. Wang, Q. Yuan, X. Yu, D. Wang, and Y. Chen, "Ag-modified porous perovskite-type $LaFeO_3$ for efficient ethanol detection," *Nanomaterials*, vol. 12, no. 10, p. 1768, 2022.

[37] R. Malik, N. Joshi, and V. K. Tomer, "Advances in the designs and mechanisms of MoO_3 nanostructures for gas sensors: a holistic review," *Materials Advances*, vol. 2, no. 13, pp. 4190–4227, 2021.

[38] N. J. Joshi, M. L. Braunger, F. M. Shimizu, A. Riul Jr., and O. N. J. M. M. de Oliveira Jr, "Insights into nano-heterostructured materials for gas sensing: a review," *Multifunctional Materials*, vol. 4, no. 3, 2021.

[39] N. Joshi, T. Hayasaka, Y. Liu, H. Liu, O. N. Oliveira Jr., and L. Lin, "A review on chemiresistive room temperature gas sensors based on metal oxide nanostructures, graphene and 2D transition metal dichalcogenides," *Microchimica Acta*, vol. 185, no. 4, p. 213, 2018.

[40] X. Liu, T. Ma, N. Pinna, and J. Zhang, "Two-dimensional nanostructured materials for gas sensing," *Advanced Functional Materials*, vol. 27, no. 37, 2017.

[41] J. Zhang, X. Liu, G. Neri, and N. J. A. Pinna, "Nanostructured materials for room-temperature gas sensors," *Advanced Materials Advanced Materials*, vol. 28, no. 5, pp. 795–831, 2016.

[42] A. Saaedi, P. Shabani, and R. Yousefi, "Study on the effects of the magneto assisted deposition on ammonia gas sensing properties of polyaniline," *Journal of Materials Science-Materials in Electronics*, vol. 30, no. 11, pp. 10765–10775, 2019.

[43] L. Zhu and W. Zeng, "Room-temperature gas sensing of ZnO-based gas sensor: a review," *Sensors and Actuators a-Physical*, vol. 267, pp. 242–261, 2017.

[44] Y. Wang, B. Liu, S. Xiao et al., "Low-temperature H_2S detection with hierarchical Cr-doped WO_3 microspheres," *ACS Applied Materials & Interfaces*, vol. 8, no. 15, pp. 9674–9683, 2016.

[45] Y. Liu, J. Bai, Y. Li et al., "Preparation of PdO-decorated NiO porous film on ceramic substrate for highly selective and sensitive H_2S detection," *Ceramics International*, vol. 48, no. 4, pp. 4787–4794, 2022.

[46] H. Liu, Z. Wang, G. Cao et al., "Construction of hollow NiO/ZnO p-n heterostructure for ultrahigh performance toluene gas sensor," *Materials Science in Semiconductor Processing*, vol. 141, p. 106435, 2022.

[47] C. Li, P. G. Choi, K. Kim, and Y. Masuda, "High performance acetone gas sensor based on ultrathin porous NiO nanosheet," *Sensors and Actuators B-Chemical*, vol. 367, p. 132143, 2022.

[48] Y. Zhang, S. Han, M. Wang et al., "Electrospun Cu-doped In_2O_3 hollow nanofibers with enhanced H2S gas sensing performance," *Journal of Advanced Ceramics*, vol. 11, no. 3, pp. 427–442, 2022.

[49] C. Zhang, Y. Huan, Y. Li, Y. Luo, and M. Debliquy, "Low concentration isopropanol gas sensing properties of Ag nanoparticles decorated In_2O_3 hollow spheres," *Journal of Advanced Ceramics*, vol. 11, no. 3, pp. 379–391, 2022.

[50] T. P. Mokoena, H. C. Swart, and D. E. Motaung, "A review on recent progress of p-type nickel oxide based gas sensors: future perspectives," *Journal of Alloys and Compounds*, vol. 805, pp. 267–294, 2019.

[51] Y. Lu, Y. H. Ma, S. Y. Ma et al., "Curly porous NiO nanosheets with enhanced gas-sensing properties," *Materials Letters*, vol. 190, pp. 252–255, 2017.

[52] S. Cao, L. Peng, B. Liu et al., "Hydrothermal synthesis of novel lotus-root slice NiO architectures with enhanced gas response properties," *Journal of Alloys and Compounds*, vol. 798, pp. 478–483, 2019.

[53] C. Su, L. Zhang, Y. Han et al., "Controllable synthesis of crescent-shaped porous NiO nanoplates for conductometric ethanol gas sensors," *Sensors and Actuators B-Chemical*, vol. 296, p. 126642, 2019.

[54] S. Liu, W. Zeng, and T. Chen, "Synthesis of hierarchical flower-like NiO and the influence of surfactant," *Physica E-Low-Dimensional Systems & Nanostructures*, vol. 85, pp. 13–18, 2017.

[55] Y. Zhang and W. Zeng, "New insight into gas sensing performance of nanoneedle-assembled and nanosheet-assembled hierarchical NiO nanoflowers," *Materials Letters*, vol. 195, pp. 217–219, 2017.

[56] M. Carbone and P. Tagliatesta, "NiO grained-flowers and nanoparticles for ethanol sensing," *Materials*, vol. 13, no. 8, p. 1880, 2020.

[57] Q. Gao, W. Zeng, and R. Miao, "Synthesis of multifarious hierarchical flower-like NiO and their gas-sensing properties," *Journal of Materials Science-Materials in Electronics*, vol. 27, no. 9, pp. 9410–9416, 2016.

[58] S. Cao, T. Han, and L. Peng, "Surfactant-free synthesis of 3D hierarchical flower-like NiO nanostructures with enhanced ethanol-sensing performance," *Journal of Materials Science-Materials in Electronics*, vol. 31, no. 20, pp. 17291–17296, 2020.

[59] J. Wang, Q. Zhou, Z. Lu, Z. Wei, and W. Zeng, "The novel 2D honeycomb-like NiO nanoplates assembled by nanosheet arrays with excellent gas sensing performance," *Materials Letters*, vol. 255, p. 126523, 2019.

[60] X. Chen, S. Wang, C. Su et al., "Two-dimensional Cd-doped porous Co_3O_4 nanosheets for enhanced room-temperature NO_2 sensing performance," *Sensors and Actuators B-Chemical*, vol. 305, p. 127393, 2020.

[61] J.-H. Kim, A. Mirzaei, M. Osada, H. W. Kim, and S. S. Kim, "Hydrogen sensing characteristics of Pd-decorated ultrathin ZnO nanosheets," *Sensors and Actuators B-Chemical*, vol. 329, p. 129222, 2021.

[62] M. Kumar, V. Bhatt, J. Kim et al., "Holey engineered 2D ZnO-nanosheets architecture for supersensitive ppm level H_2 gas detection at room temperature," *Sensors and Actuators B-Chemical*, vol. 326, p. 128839, 2021.

[63] Y.-C. Liang, Y.-C. Chang, and W.-C. Zhao, "Design and synthesis of novel 2D porous zinc oxide-nickel oxide composite nanosheets for detecting ethanol vapor," *Nanomaterials*, vol. 10, no. 10, p. 1989, 2020.

[64] R. S. Ganesh, G. K. Mani, R. Elayaraja et al., "ZnO hierarchical 3D-flower like architectures and their gas sensing properties at room temperature," *Applied Surface Science*, vol. 449, pp. 314–321, 2018.

[65] A. Das, P. M. Kumar, M. Bhagavathiachari, and R. G. Nair, "Shape selective flower-like ZnO nanostructures prepared via structure- directing reagent free methods for efficient photocatalytic performance," *Materials Science and Engineering B-Advanced Functional Solid-State Materials*, vol. 269, p. 115149, 2021.

[66] L. Song, A. Lukianov, D. Butenko et al., "Facile synthesis of hierarchical tin oxide nanoflowers with ultra-high methanol gas sensing at low working temperature," *Nanoscale Research Letters*, vol. 14, no. 1, p. 84, 2019.

[67] R. G. Motsoeneng, I. Kortidis, R. Rikhotso, H. C. Swart, S. S. Ray, and D. E. Motaung, "Temperature-dependent response to C_3H_7OH and C_2H_5OH vapors induced by deposition of Au nanoparticles on SnO_2/NiO hollow sphere-based conductometric sensors," *Sensors and Actuators B-Chemical*, vol. 316, p. 128041, 2020.

[68] X. Wang, F. Liu, X. Chen et al., "SnO_2 core-shell hollow microspheres co-modification with Au and NiO nanoparticles for acetone gas sensing," *Powder Technology*, vol. 364, pp. 159–166, 2020.

[69] Q. Hu, Z. Wang, J. Chang, P. Wan, J. Huang, and L. Feng, "Design and preparation of hollow NiO sphere- polyaniline composite for NH_3 gas sensing at room temperature," *Sensors and Actuators B-Chemical*, vol. 344, p. 130179, 2021.

[70] J. Yang, W. Han, J. Ma et al., "Sn doping effect on NiO hollow nanofibers based gas sensors about the humidity dependence for triethylamine detection," *Sensors and Actuators B-Chemical*, vol. 340, p. 129971, 2021.

[71] W.-C. Geng, X.-R. Cao, S.-L. Xu et al., "Synthesis of hollow spherical nickel oxide and its gas-sensing properties," *Rare Metals*, vol. 40, no. 6, pp. 1622–1631, 2021.

[72] S. Bai, H. Fu, X. Shu et al., "NiO hierarchical hollow microspheres doped Fe to enhance triethylamine sensing properties," *Materials Letters*, vol. 210, pp. 305–308, 2018.

[73] S. Chu, C. Yang, and X. Su, "Synthesis of NiO hollow nanospheres via Kirkendall effect and their enhanced gas sensing performance," *Applied Surface Science*, vol. 492, pp. 82–88, 2019.

[74] L. Wei, Y. Xia, and J. Meng, "A novel hollow nickel oxide sensor and gas detection performance in asphalt," *Science of Advanced Materials*, vol. 11, no. 1, pp. 56–59, 2019.

[75] C. Kuang, W. Zeng, H. Ye, and Y. Li, "A novel approach for fabricating NiO hollow spheres for gas sensors," *Physica E-Low-Dimensional Systems & Nanostructures*, vol. 97, pp. 314–316, 2018.

[76] B. Liu, M. Wang, S. Liu, H. Zheng, and H. Yang, "The sensing reaction on the Ni-NiO (111) surface at atomic and molecule level and migration of electron," *Sensors and Actuators B-Chemical*, vol. 273, pp. 794–803, 2018.

[77] B. Liu, L. Wang, Y. Ma et al., "Enhanced gas–sensing properties and sensing mechanism of the foam structures assembled from NiO nanoflakes with exposed {1 1 1} facets," *Applied Surface Science*, vol. 470, pp. 596–606, 2019.

[78] Y. Liang, Y. Yang, H. Zhou et al., "Active {111}-faceted ultrathin NiO single-crystalline porous nanosheets supported highly dispersed Pt nanoparticles for synergetic enhancement of gas sensing and photocatalytic performance," *Applied Surface Science*, vol. 471, pp. 124–133, 2019.

[79] A. Hermawan, A. T. Hanindriyo, E. R. Ramadhan et al., "Octahedral morphology of NiO with (111) facet synthesized from the transformation of NiOHCl for the NOx detection and degradation: experiment and DFT calculation," *Inorganic Chemistry Frontiers*, vol. 7, no. 18, pp. 3431–3442, 2020.

[80] B. Deng, J. Jiang, H. Li et al., "Enhanced piezoelectric property in Mn-doped $K_{0.5}Na_{0.5}NbO_3$ ceramics via cold sintering process and KMnO4 solution," *Journal of the American Ceramic Society*, vol. 105, no. 9, pp. 5774–5782, 2022.

[81] Z. Peng, L. Chen, Y. Xiang, and F. Cao, "Microstructure and electrical properties of lanthanides-doped $CaBi_2Nb_2O_9$ ceramics," *Materials Research Bulletin*, vol. 148, p. 111670, 2022.

[82] C. Wang, X. Cui, J. Liu et al., "Design of superior ethanol gas sensor based on Al-doped NiO nanorod-flowers," *Acs Sensors*, vol. 1, no. 2, pp. 131–136, 2016.

[83] L. Zhu, W. Zeng, J. Yang, and Y. Li, "Unique hierarchical Ce-doped NiO microflowers with enhanced gas sensing performance," *Materials Letters*, vol. 251, pp. 61–64, 2019.

[84] Q. Wang, J. Bai, Q. Hu et al., "W-doped NiO as a material for selective resistive ethanol sensors," *Sensors and Actuators B-Chemical*, vol. 308, p. 127668, 2020.

[85] J. Y. Niu, L. Wang, B. Hong et al., "Synergistic effects of α-Fe2O3nanoparticles and Fe-doping on gas-sensing performance of NiO nanowires and interface mechanism," *Nanotechnology*, vol. 32, no. 48, p. 485502, 2021.

[86] J. Wei, X. Li, Y. Han et al., "Highly improved ethanol gas-sensing performance of mesoporous nickel oxides nanowires with the stannum donor doping," *Nanotechnology*, vol. 29, no. 24, p. 245501, 2018.

[87] M. Taeno, D. Maestre, and A. Cremades, "Fabrication and study of self-assembled NiO surface networks assisted by Sn doping," *Journal of Alloys and Compounds*, vol. 827, p. 154172, 2020.

[88] S. Shailja, K. J. Singh, and R. C. Singh, "Highly sensitive and selective ethanol gas sensor based on Ga-doped NiO nanoparticles," *Journal of Materials Science-Materials in Electronics*, vol. 32, no. 8, pp. 11274–11290, 2021.

[89] Z. Zhang, Z. Wen, S. Khan, N. Rahman, and L. Zhu, "Humidity sensor based on mesoporous Al-doped NiO ultralong nanowires with enhanced ethanol sensing performance," *Journal of Materials Science-Materials in Electronics*, vol. 30, no. 7, pp. 7121–7134, 2019.

[90] H. D. Chen, K. L. Jin, J. C. Xu et al., "High-valence cations-doped mesoporous nickel oxides nanowires: nanocasting synthesis, microstructures and improved gas-sensing performance," *Sensors and Actuators B-Chemical*, vol. 296, p. 126622, 2019.

[91] J. Chang, M. Horprathum, D. Wang et al., "Aliovalent Sc and Li co-doping boosts the performance of p-type NiO sensor," *Sensors and Actuators B-Chemical*, vol. 326, p. 128834, 2021.

[92] X. Sun, X. Hu, Y. Wang et al., "Enhanced gas-sensing performance of Fe-doped ordered mesoporous NiO with long-range periodicity," *Journal of Physical Chemistry C*, vol. 119, no. 6, pp. 3228–3237, 2015.

[93] Y. Zhao, J. Yan, Y. Huang et al., "Interfacial self-assembly of monolayer Mg-doped NiO honeycomb structured thin film with enhanced performance for gas sensing," *Journal of Materials Science-Materials in Electronics*, vol. 29, no. 13, pp. 11498–11508, 2018.

[94] Y. Tang, Z. Han, Y. Qi et al., "Enhanced ppb-level formaldehyde sensing performance over Pt deposited SnO_2 nanospheres," *Journal of Alloys and Compounds*, vol. 899, p. 163230, 2022.

[95] S. M. Majhi, G. K. Naik, H.-J. Lee et al., "Au@NiO core-shell nanoparticles as a p-type gas sensor: novel synthesis, characterization, and their gas sensing properties with sensing mechanism," *Sensors and Actuators B-Chemical*, vol. 268, pp. 223–231, 2018.

[96] J. Fu, C. Zhao, J. Zhang, Y. Peng, and E. Xie, "Enhanced gas sensing performance of electrospun Pt-functionalized NiO nanotubes with chemical and electronic sensitization," *ACS Applied Materials & Interfaces*, vol. 5, no. 15, pp. 7410–7416, 2013.

[97] S. Park, H. Kheel, G.-J. Sun, S. K. Hyun, S. E. Park, and C. Lee, "Ethanol sensing properties of Au-functionalized NiO nanoparticles," *Bulletin of the Korean Chemical Society*, vol. 37, no. 5, pp. 713–719, 2016.

[98] S.-C. Wang, X.-H. Wang, G.-Q. Qiao et al., "NiO nanoparticles-decorated ZnO hierarchical structures for isopropanol gas sensing," *Rare Metals*, vol. 41, no. 3, pp. 960–971, 2022.

[99] J. Zhang and J. Li, "The oxygen vacancy defect of ZnO/NiO nanomaterials improves photocatalytic performance and ammonia sensing performance," *Nanomaterials*, vol. 12, no. 3, p. 433, 2022.

[100] H.-F. Bao, T.-T. Yue, X.-X. Zhang, Z. Dong, Y. Yan, and W. Feng, "Enhanced ethanol-sensing properties based on modified NiO-ZnO p-n heterojunction nanotubes," *Journal of Nanoscience and Nanotechnology*, vol. 20, no. 2, pp. 731–740, 2020.

[101] L. Zhu, W. Zeng, J. Yang, and Y. Li, "Fabrication of hierarchical hollow NiO/ZnO microspheres for ethanol sensing property," *Materials Letters*, vol. 230, pp. 297–299, 2018.

[102] L. Zhu, W. Zeng, J. Yang, and Y. Li, "One-step hydrothermal fabrication of nanosheet-assembled NiO/ZnO microflower and its ethanol sensing property," *Ceramics International*, vol. 44, no. 16, pp. 19825–19830, 2018.

[103] L. Qiu, W. Zeng, Y. Li, and Q. Zhou, "Synthesis of nanosheet-assembled porous NiO/ZnO microflowers through a facile one-step hydrothermal approach," *Materials Letters*, vol. 256, p. 126649, 2019.

[104] H. Chen, R. Bo, A. Shrestha et al., "NiO-ZnO nanoheterojunction networks for room-temperature volatile organic compounds sensing," *Advanced Optical Materials*, vol. 6, no. 22, p. 1800677, 2018.

[105] S. T. Hezarjaribi and S. Nasirian, "An enhanced fast ethanol sensor based on zinc oxide/nickel oxide nanocomposite in dynamic situations," *Journal of Inorganic and Organometallic Polymers and Materials*, vol. 30, no. 10, pp. 4072–4081, 2020.

[106] X. Deng, L. Zhang, J. Guo, Q. Chen, and J. Ma, "ZnO enhanced NiO-based gas sensors towards ethanol," *Materials Research Bulletin*, vol. 90, pp. 170–174, 2017.

[107] C. Baratto, R. Kumar, E. Comini, M. Ferroni, and M. Campanini, "Bottle-brush-shaped heterostructures of NiO-ZnO nanowires: growth study and sensing properties," *Nanotechnology*, vol. 28, no. 46, p. 465502, 2017.

[108] J. Bai, C. Zhao, H. Gong et al., "Debye-length controlled gas sensing performances in NiO@ZnO p-n junctional core-shell nanotubes," *Journal of Physics D-Applied Physics*, vol. 52, no. 28, p. 285103, 2019.

[109] L. Zhou, W. Zeng, and Y. Li, "A facile one-step hydrothermal synthesis of a novel NiO/ZnO nanorod composite and its enhanced ethanol sensing property," *Materials Letters*, vol. 254, pp. 92–95, 2019.

[110] S. Zhao, Y. Shen, Y. Xia et al., "Synthesis and gas sensing properties of NiO/ZnO heterostructured nanowires," *Journal of Alloys and Compounds*, vol. 877, p. 160189, 2021.

[111] N. Jayababu, M. Poloju, J. Shruthi, and M. V. R. Reddy, "Semi shield driven p-n heterostructures and their role in enhancing the room temperature ethanol gas sensing performance of NiO/SnO2 nanocomposites," *Ceramics International*, vol. 45, no. 12, pp. 15134–15142, 2019.

[112] Y. Chu, H. Liu, and S. Yan, "Preparation and gas sensing properties of SnO_2/NiO composite semiconductor

nanofibers," *Journal of Inorganic Materials*, vol. 36, no. 9, pp. 950–958, 2021.

[113] S. U. Din, M. Ul Haq, M. Sajid et al., "Development of high-performance sensor based on NiO/SnO2heterostructures to study sensing properties towards various reducing gases," *Nanotechnology*, vol. 31, no. 39, p. 395502, 2020.

[114] W. Tong, Y. Wang, Y. Bian, A. Wang, N. Han, and Y. Chen, "Sensitive cross-linked SnO_2:NiO networks for MEMS compatible ethanol gas sensors," *Nanoscale Research Letters*, vol. 15, no. 1, p. 35, 2020.

[115] L. Zhang, J. He, and W. Jiao, "Synthesis and gas sensing performance of NiO decorated SnO_2 vertical-standing nanotubes composite thin films," *Sensors and Actuators B-Chemical*, vol. 281, pp. 326–334, 2019.

[116] J. He, W. Jiao, L. Zhang, and R. Feng, "Preparation and gas-sensing performance of SnO_2/NiO composite oxide synthesized by microwave-assisted liquid phase deposition," *Particuology*, vol. 41, pp. 118–125, 2018.

[117] G. Niu, C. Zhao, H. Gong, Z. Yang, X. Leng, and F. Wang, "NiO nanoparticle-decorated SnO_2 nanosheets for ethanol sensing with enhanced moisture resistance," *Microsystems & Nanoengineering*, vol. 5, no. 1, p. 21, 2019.

[118] G. Sun, H. Chen, Y. Li et al., "Synthesis and improved gas sensing properties of NiO-decorated SnO_2 microflowers assembled with porous nanorods," *Sensors and Actuators B-Chemical*, vol. 233, pp. 180–192, 2016.

[119] Z. Wei, Q. Zhou, J. Wang, and W. Zeng, "Hydrothermal synthesis of hierarchical WO_3/NiO porous microsphere with enhanced gas sensing performances," *Materials Letters*, vol. 264, p. 127383, 2020.

[120] F.-R. Juang and W.-Y. Wang, "Ethanol gas sensors with nanocomposite of nickel oxide and tungsten oxide," *IEEE Sensors Journal*, vol. 21, no. 18, pp. 19740–19752, 2021.

[121] L. Lin, T. Liu, Y. Zhang, S. Hussain, S. Wu, and W. Zeng, "Superior ethanol-sensing performance research of WO_3 center dot $0.33H_{(2)}O$ doped chrysanthemum-like NiO composite," *Materials Letters*, vol. 108, pp. 231–234, 2013.

[122] L. Wang, B. Hong, H. D. Chen et al., "The highly improved gas-sensing performance of α-Fe2O3-decorated NiO nanowires and the interfacial effect of p-n heterojunctions," *Journal of Materials Chemistry C*, vol. 8, no. 11, pp. 3855–3864, 2020.

[123] S. Dong, D. Wu, W. Gao, H. Hao, G. Liu, and S. Yan, "Multi-dimensional templated synthesis of hierarchical Fe_2O_3/NiO composites and their superior ethanol sensing properties promoted by nanoscale p-n heterojunctions," *Dalton Transactions*, vol. 49, no. 4, pp. 1300–1310, 2020.

[124] W. Tan, J. Tan, L. Fan, Z. Yu, J. Qian, and X. Huang, "Fe_2O_3-loaded NiO nanosheets for fast response/recovery and high response gas sensor," *Sensors and Actuators B-Chemical*, vol. 256, pp. 282–293, 2018.

[125] S. Yan, W. Song, D. Wu et al., "Assembly of In_2O_3 nanoparticles decorated NiO nanosheets heterostructures and their enhanced gas sensing characteristics," *Journal of Alloys and Compounds*, vol. 896, p. 162887, 2022.

[126] H.-J. Kim, H.-M. Jeong, T.-H. Kim, J.-H. Chung, Y. C. Kang, and J.-H. Lee, "Enhanced ethanol sensing characteristics of In_2O_3-decorated NiO hollow nanostructures via modulation of hole accumulation layers," *ACS Applied Materials & Interfaces*, vol. 6, no. 20, pp. 18197–18204, 2014.

[127] J. Lee, Y. Choi, B. J. Park et al., "Precise control of surface oxygen vacancies in ZnO nanoparticles for extremely high acetone sensing response," *Journal of Advanced Ceramics*, vol. 11, no. 5, pp. 769–783, 2022.

[128] X. Tian, H. Cao, X. Wei, J. Wang, X. Wu, and H. Wang, "Controllable acid vapor oxidation growth of complex SnO_2 nanostructures for ultrasensitive ethanol sensing," *Ceramics International*, vol. 48, no. 7, pp. 9229–9238, 2022.

[129] Y. Zhang, Z. Yang, L. Zhao, T. Fei, S. Liu, and T. Zhang, "Boosting room-temperature ppb-level NO_2 sensing over reduced graphene oxide by co-decoration of α-Fe_2O_3 and SnO_2 nanocrystals," *Journal of Colloid and Interface Science*, vol. 612, pp. 689–700, 2022.

[130] J. N. Mao, B. Hong, H. D. Chen et al., "Highly improved ethanol gas response of n-type α-Fe_2O_3 bunched nanowires sensor with high-valence donor-doping," *Journal of Alloys and Compounds*, vol. 827, p. 154248, 2020.

[131] X. Chen, R. Liang, C. Qin, Z. Ye, and L. Zhu, "Coaxial electrospinning Fe_2O_3@Co_3O_4 double-shelled nanotubes for enhanced ethanol sensing performance in a wide humidity range," *Journal of Alloys and Compounds*, vol. 891, p. 161868, 2022.

[132] W.-H. Zhang, S.-J. Ding, Q.-S. Zhang et al., "Rare earth element-doped porous In_2O_3 nanosheets for enhanced gas-sensing performance," *Rare Metals*, vol. 40, no. 6, pp. 1662–1668, 2021.

[133] H.-L. Yu, J. Wang, B. Zheng et al., "Fabrication of single crystalline WO_3 nano-belts based photoelectric gas sensor for detection of high concentration ethanol gas at room temperature," *Sensors and Actuators a-Physical*, vol. 303, p. 111865, 2020.

[134] D. Zhang, Y. Cao, J. Wu, and X. Zhang, "Tungsten trioxide nanoparticles decorated tungsten disulfide nanoheterojunction for highly sensitive ethanol gas sensing application," *Applied Surface Science*, vol. 503, p. 144063, 2020.

[135] J. Gao, C. Liu, S. Guo, L. Yang, Y. Yang, and K. Xu, "Heteroepitaxy growth of cobalt oxide/nickel oxide nanowire arrays on alumina substrates for enhanced ethanol sensing characteristics," *Ceramics International*, vol. 48, no. 3, pp. 3849–3859, 2022.

[136] P. Hao, Z. Lin, P. Song, Z. Yang, and Q. Wang, "rGO-wrapped porous $LaFeO_3$ microspheres for high-performance triethylamine gas sensors," *Ceramics International*, vol. 46, no. 7, pp. 9363–9369, 2020.

[137] Z. Ma, K. Yang, C. Xiao, and L. Jia, "C-doped $LaFeO_3$ porous nanostructures for highly selective detection of formaldehyde," *Sensors and Actuators B-Chemical*, vol. 347, p. 130550, 2021.

[138] P. Hao, G. Qiu, P. Song, Z. Yang, and Q. Wang, "Construction of porous $LaFeO_3$ microspheres decorated with NiO nanosheets for high response ethanol gas sensors," *Applied Surface Science*, vol. 515, p. 146025, 2020.

[139] M. Haq, Z. Zhang, X. Chen et al., "A two-step synthesis of microsphere-decorated fibers based on NiO/$ZnSnO_3$ composites towards superior ethanol sensitivity performance," *Journal of Alloys and Compounds*, vol. 777, pp. 73–83, 2019.